AFRL-AFOSR-UK-TR-2021-0018

Mechanical and Impact Properties of Structural Power Devices

Greenhalgh, Emile
IMPERIAL COLLEGE OF SCIENCE TECHNOLOGY & MEDICINE
EXHIBITION RD
LONDON, ,
GB

06/25/2021
Final Technical Report

Air Force Research Laboratory
Air Force Office of Scientific Research
European Office of Aerospace Research and Development
Unit 4515 Box 14, APO AE 09421

REPORT DOCUMENTATION PAGE

Form Approved
OMB No. 0704-0188

1. REPORT DATE *(DD-MM-YYYY)*	**2. REPORT TYPE**	**3. DATES COVERED** *(From - To)*
25-06-2021	Final	01 Sep 2017 - 31 Aug 2020

4. TITLE AND SUBTITLE
Mechanical and Impact Properties of Structural Power Devices

5a. CONTRACT NUMBER

5b. GRANT NUMBER
FA9550-17-1-0251

5c. PROGRAM ELEMENT NUMBER

6. AUTHOR(S)
Emile Greenhalgh

5d. PROJECT NUMBER

5e. TASK NUMBER

5f. WORK UNIT NUMBER

7. PERFORMING ORGANIZATION NAME(S) AND ADDRESS(ES)
IMPERIAL COLLEGE OF SCIENCE TECHNOLOGY & MEDICINE
EXHIBITION RD
LONDON,
GB

8. PERFORMING ORGANIZATION REPORT NUMBER

9. SPONSORING/MONITORING AGENCY NAME(S) AND ADDRESS(ES)
EOARD
UNIT 4515
APO AE 09421-4515

10. SPONSOR/MONITOR'S ACRONYM(S)
AFRL/AFOSR IOE

11. SPONSOR/MONITOR'S REPORT NUMBER(S)
AFRL-AFOSR-UK-TR-2021-0018

12. DISTRIBUTION/AVAILABILITY STATEMENT
A Distribution Unlimited: PB Public Release

13. SUPPLEMENTARY NOTES

14. ABSTRACT
This report contains the details and results of multifunctional composite material for electrical energy storage and structural loads. Structural Power Composites. The study was to understand basic material behavior, simultaneously improve mechanical and electrical performance, and damage behavior. The research objectives were met.

15. SUBJECT TERMS

16. SECURITY CLASSIFICATION OF:			**17. LIMITATION OF ABSTRACT**	**18. NUMBER OF PAGES**	**19a. NAME OF RESPONSIBLE PERSON**
a. REPORT	**b. ABSTRACT**	**c. THIS PAGE**			DAVID GARNER
U	U	U	SAR	31	**19b. TELEPHONE NUMBER** *(Include area code)* 314-235-6420

Final Technical Report (June 2021)

Damage Tolerance & Durability of Structural Power Composites (Award FA9550-17-1-0251)

Imperial College London

E.S Greenhalgh, Maria Francesca Pernice, Guocheng Qi, Evgeny Senokos, David B. Anthony, Sang Nguyen, Maria Valkova, Milo S. P. Shaffer, Anthony R. J. Kucernak

Table of Contents

Summary

This is a technical report on the work performed at Imperial College London, UK under the award no. FA9550-17-1-0251 during the time period 2017-10-01 to 2020-08-30. It covers descriptions of the work performed and the associated publications.

The work was focused on addressing issues associated with the development and maturation of structural supercapacitors. The work we have undertaken has been partitioned into constituent development, device manufacture, device characterisation, multifunctional modelling and design, and demonstration. The research undertaken in each of these areas is reported here.

The research has culminated in fifteen journal papers and six conference papers completely or partly funded by this AFOSR/EOARD grant. Some of the work has been done in collaboration with The Royal Institute of Technology (KTH) in Stockholm and Chalmers University in Gothenburg.

The Team

This project has been conducted as part of a larger portfolio of projects run by an interdisciplinary team at Imperial College London headed by Prof. Greenhalgh. All together three academics, three Ph.D.-students and seven post-docs have been involved (Figure 1).

Figure 1 Structural power team at Imperial College London.

Highlights and Achievements

Over the three year project, the following was achieved:

- Scale-up and optimisation of the CAG process, and the coating of the CAG with active material (MnO_2) to enhance the electrochemical performance;
- Identification that the CAG process depresses the tensile strength, and investigation into mitigation strategies to address this issue;
- Refinement of the device manufacturing process, including separator selection and investigation of the influence of manufacturing parameters on the electrochemical performance of structural supercapacitors;
- Studies into encapsulation strategies for structural supercapacitors, and investigation into their integration into multicell components;
- Mechanical (tensile and in-plane shear) characterization of structural supercapacitors to provide a comparison between multifunctional and monofunctional equivalents;
- Investigation into current collection and optimization of the material selection and geometry to minimize the resistive losses in structural supercapacitors;
- Development of multiphysics, multifunctional predictive models for structural supercapacitors, including consolidation prediction of the devices, mechanical modelling (principally elastic behaviour) and electrochemical modelling;
- Development and delivery of a multifunctional design methodology, and analysis of adoption strategies for various vehicles, such as an aircraft cabin, fully electric airliner and an electric airtaxi;
- Demonstration of a multicell assembly to power opening of an aircraft cabin door.

Constituent Development

The development of constituents (such as structural electrodes, structural electrolytes and structural separators) underpins the scientific advance of structural power. Over the course of this project we have focussed on development of carbon aerogel coated carbon fibre (CF/CAG) structural electrodes, which had been initiated by background research at ICL. The CAG's stiff bi-continuous 3D structure provides lateral support to the carbon fibres under shear and compressive loading. This reinforcement development work (see Figure 2) was accomplished before this project, with the CF/CAG preparation methodologies, specific surface areas and morphologies were reported elsewhere [14].

Over the course of this project the CAG modification process was further improved [15]. Firstly, the reinforcements were scaled up: CF/CAG can currently be produced as 30 × 20 cm² sheets to enable a combination of standard coupon testing and electrochemical characterisation, though this size could be further scaled up by using a larger pyrolysis furnace. Secondly, the morphology and microstructure of the woven fabric was maintained throughout the aerogel process allowing the infusion of different CF fabrics, from plain, biaxial, unidirectional non-crimp fabrics (NCF) fabrics to more complicated fibre architectures or preforms. Thirdly, precursor-aged samples are carbonised at 800 °C to produce an electrically conductive, porous, high surface area structural supercapacitor electrode. This pyrolysis process can potentially damage the fibres; hence efforts to lower the temperatures required for pyrolysis are being investigated.

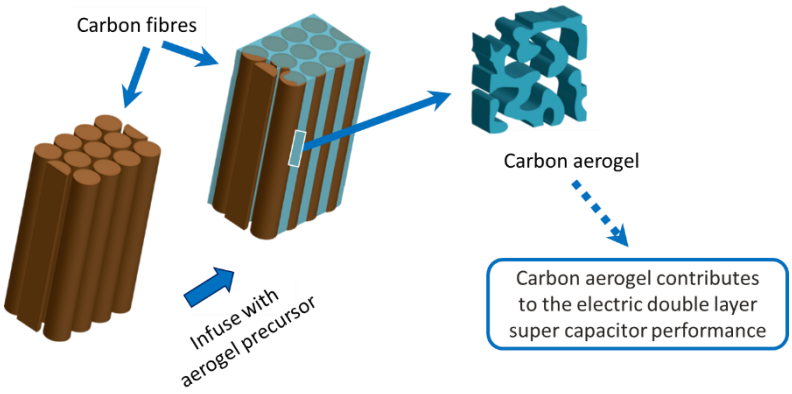

Figure 2 Schematic of the route to achieving a high surface area CF/CAG reinforcement.

In terms of the multifunctional electrolyte, a combination of epoxy and aqueous solutions or ionic liquids were used to achieve structural power, in which the epoxy offers mechanical load carrying capacity and aqueous solutions/ionic liquids provide ion conduction [18]. Regarding the separator, different types of insulating fabrics and non-wovens have been tested, which allow ion transport while maintaining insulation between the two porous electrodes. A good interface between the structural electrolyte and separator is desirable.

Development led to a new formulation of the carbon aerogel precursor (Figure 3), by mixing formaldehyde and resorcinol in deionised water. Potassium hydroxide was used to initiate the polymerisation process in this RF solution, and when there was sufficient viscosity the mixture was degassed and infused into dry woven CF lamina. Several materials were considered including Chromorat uniweave (C-PLY™ SP UD 100 gsm), plain (C-WEAVE™ 200P 3K HS) and spread-tow NCF (C-PLY™ BX 100 gsm), as well as Textreme spread tow plain weave (TeXtreme UTS50 12k F2, tow width 25 mm, 64 and 43 gsm). The RIFT process was used to infuse the aerogel (RF) precursor. Following infusion, the RF was aged at elevated temperature. Then solvent exchange was used to increase the surface activation and the infused lamina were

pyrolised in an inert environment (N_2) at 800°C in a box furnace.

To further enhance the performance of these lamina studies were undertaken to introduce pseudo-capacitive elements into the electrodes [15]. CF-CAG laminae were soaked in an aqueous solution of $KMnO_4$, rinsed with de-ionised water and acetone, and then dried. The length of the soaking time and temperature dictated the resulting coating on the fibres. The resulting reinforcement plies from these synthesis processes were characterised using scanning electron microscopy and electrochemical tested in three- and two-electrode configurations, using cyclic voltammetry, electrochemical impedance spectroscopy and galvanostatic cycling (chronopotentiometry).

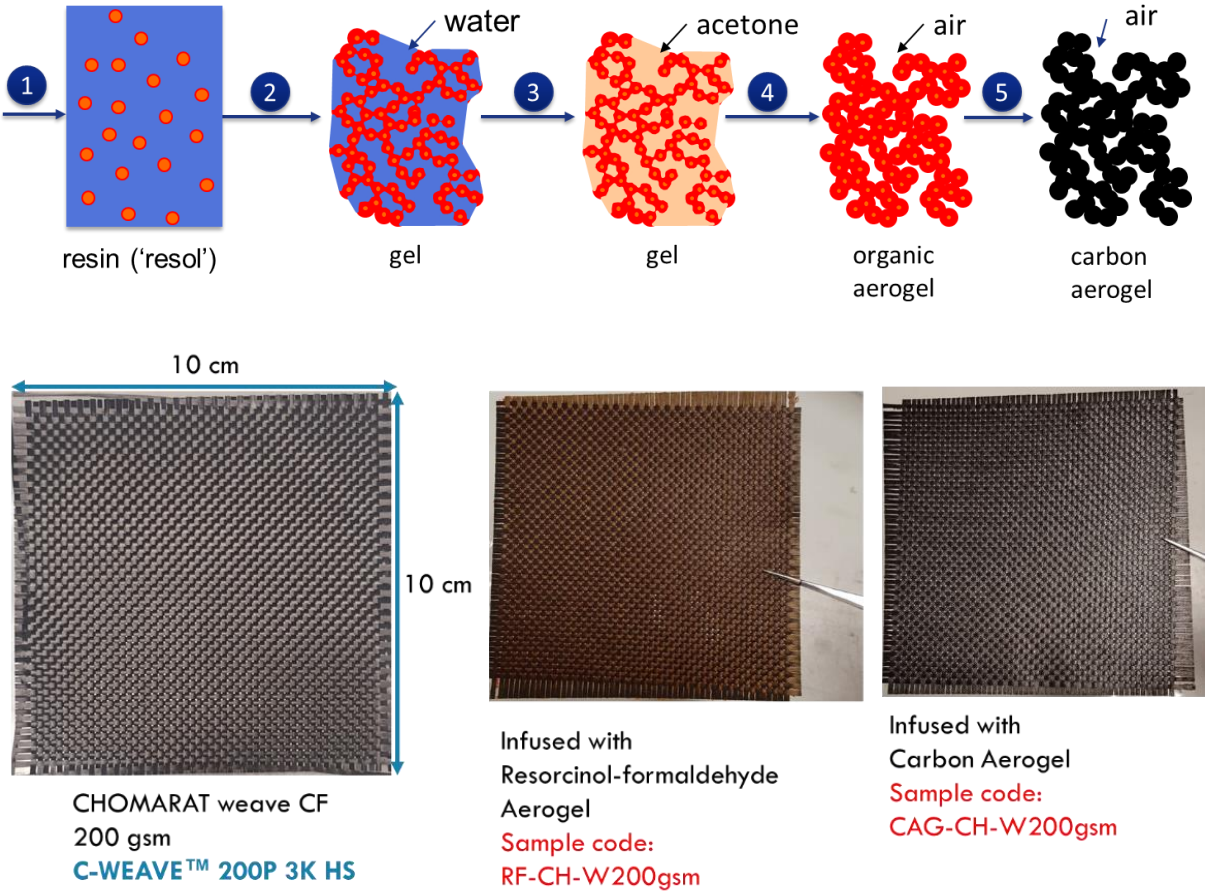

Figure 3 Top: schematic of the process by which the CF-CAG lamina were fabricated; (1) resin preparation; (2) sol-gel reaction; (3) solvent exchange in acetone; (4) drying; (5) carbonisation at 800C. Below: examples of lamina following infusion.

The electron microscopy demonstrated that the CAG coverage of the carbon fibres was good and there appeared to have been good adhesion, as shown in Figure 4. However, difficulties arose with the Textreme spread tow (bottom right in Figure 4) because the binder left a residue on the surface of the plies, which then masked the CAG process.

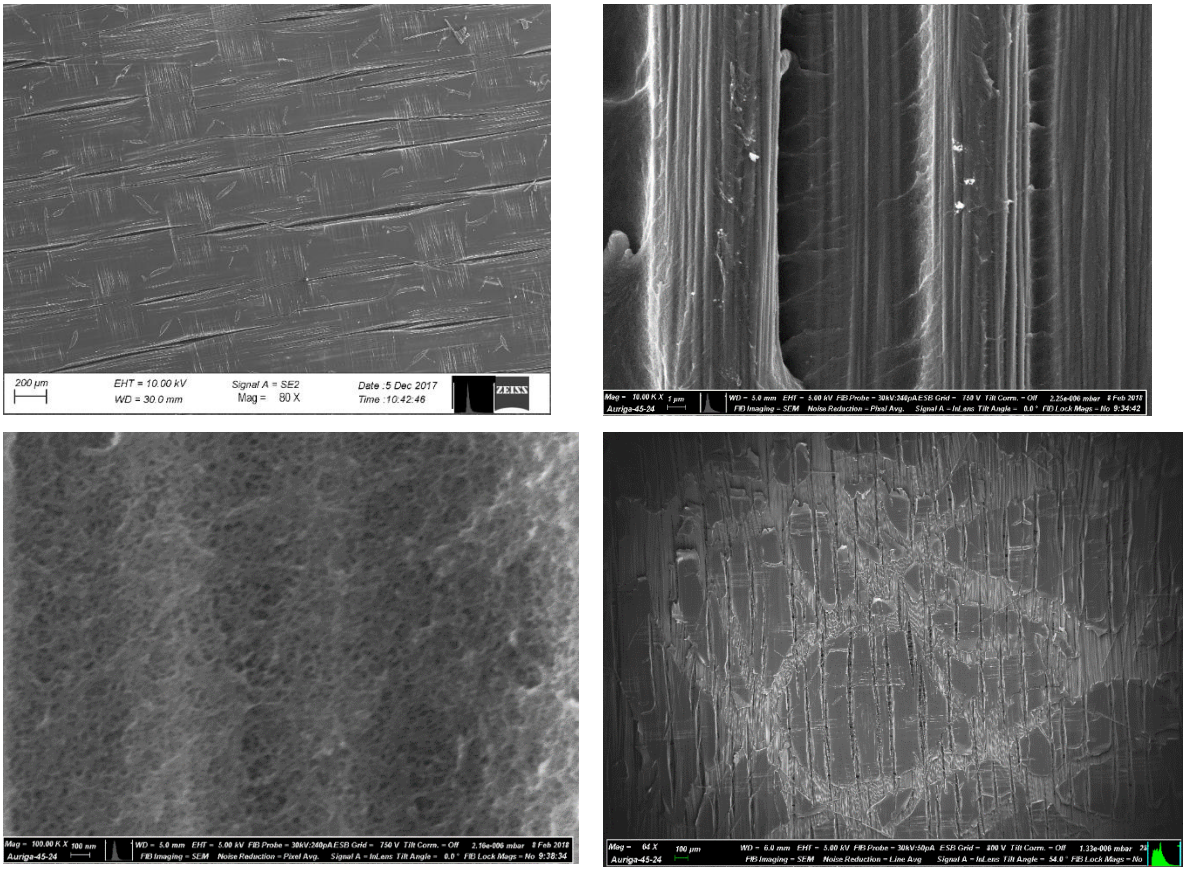

Figure 4 Exemplar scanning electron micrographs of CF-CAG lamina

A summary of the surface areas is presented in Table 1. For comparison, unmodified carbon fibres have a BET specific surface area of 0.21 m^2g^{-1} and pore volume of 0.0003 cm^3g^{-1}. The spread-tow lamina presented the highest specific surface areas.

The addition of conductive additives (CNTs, graphite nanoplatelets, and carbon black) may be beneficial to the electrochemical capacitance. Such additives may further mechanically reinforce the CAG network. However, filtering/agglomeration of the additives was observed following preliminary studies. In parallel with the CF/CAG development, a strategy to enhance capacitive capabilities of structural electrodes was explored through electrochemical deposition of pseudocapacitive manganese dioxide (MnO_2) onto high surface area CAG-modified CF fabrics [5,16]. The incorporation of MnO_2 (Figure 5a) led to a hybrid composite electrode offering significant contribution of redox reactions to the charge storage mechanism, thus enhancing the total capacitance of the system. An electrochemical deposition method based on pulse potentiometry was applied to produce MnO_2 nanowires coated onto CF/CAG composite electrodes. Electrochemical properties of CF/CAG/MnO_2 were evaluated in half and full cell and compared to as-produced CF/CAG fabrics. Symmetric SC device based on hybrid electrodes exhibited a nearly four times increase in specific capacitance (47 F/g) and energy density (1.66 Wh/kg) in 1 M Na_2SO_4 electrolyte (Figure 5b), while presenting half the power density (260 W/kg). The study demonstrated a simple route to maximize the capacitive performance of multifunctional structural supercapacitors which can be further tuned by adjusting the parameters of electrochemical deposition including deposition time, peak current density, duty cycle etc.

Table 1 Summary of BET results for CF-CAG lamina

Sample	BET SSA (m^2/g) CAG+CF	Pore volume (cm^3/g) CAG+CF	BET SSA CAG	Pore volume (cm^3/g) CAG
CAG-TeXtreme-1 (OXEON AB TeXtreme UTS50 12k F2, tow width 25 mm) - 64 gsm	192.2 ± 0.69	0.2041	835.8 ± 3.02	0.89
CAG-TeXtreme-2 (OXEON AB TeXtreme UTS50 12k F2, tow width 25 mm) - 43 gsm	237.3 ± 0.30	0.3512	1078.6 ± 1.37	1.60
CAG-C-Weave Plain (CHOMARAT C-WEAVE™ 200P 3K HS)	119.7 ± 0.11	0.2336	704.0 ± 0.11	1.37
CAG-biaxial (CHOMARAT C-PLY™ BX 100 gsm)	133.9 ± 0.14	0.1517		
CAG-UD (CHOMARAT C-PLY™ SP UD 100 gsm)	137.3 ± 0.15	0.1924		

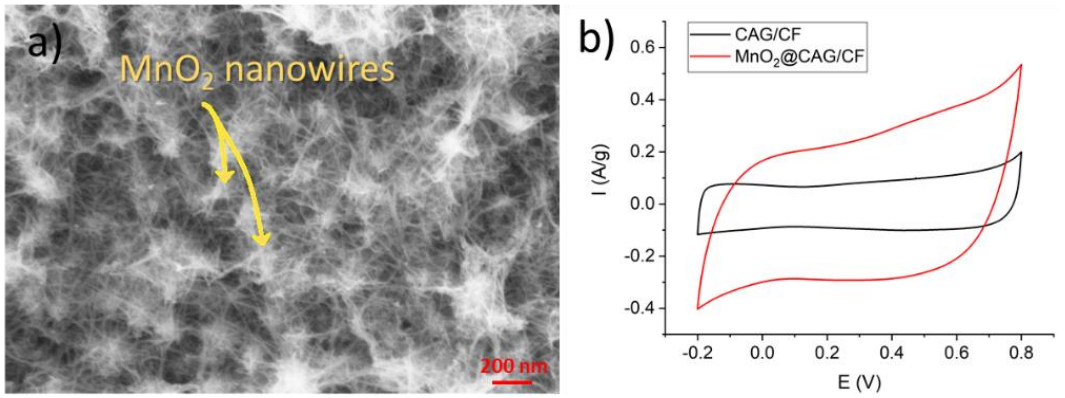

Figure 5 a) SEM image showing the morphology of MnO_2 coated CAG/CF electrode and b) CV curves at 5 mV/s comparing capacitive performance of as-produced and MnO2-modified CF/CAG.

The current method of CAG fabrication includes a carbonisation step at 800 °C which is crucial for achieving high conductivity and surface area. Such high temperature processing of CFs is inefficient and potentially can lead to degradation of the CFs and thus the mechanical properties. Furthermore, it has been shown that the microporosity of CAG can inhibit ion diffusion and restrict deposition of pseudocapacitive elements. From this perspective, work has been focused on development of alternative functional electrode materials produced at low temperatures. The study included various chemical and electrochemical methods of CF

functionalization and deposition of pseudocapacitive polyaniline (PANI) through an electrochemical polymerization process. The specific capacitance of the CF/PANI hybrid electrode was significantly enhanced as compared to carbon aerogel-modified CFs (Figure 6), although its rate capability was low. Further improvement may be achieved by forming an interconnected network of nanocarbons serving as highly conductive substrate for PANI nanostructures.

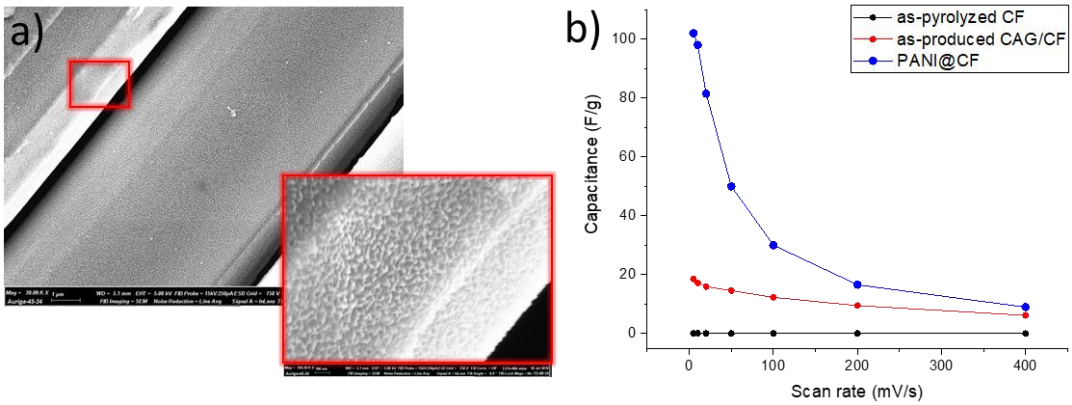

Figure 6 a) SEM image of PANI coated on pulse oxidized CF electrodes and b) capacitance versus scan rate for as-pyrolysed CF, CF/CAG and CF/PANI electrodes.

Device Manufacture

Although much of the focus of the research to date has been to develop superior reinforcements, work has been undertaken to optimise the device architecture, and particularly develop the separators for the devices [17].

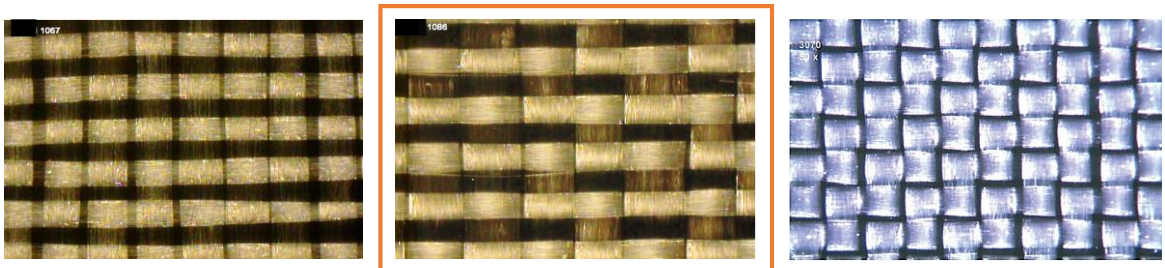

1067: 31 gsm, 32 µm thick | **1086:** 54 gsm, 50 µm thick | **3070:** 93 gsm, 86 µm thick

Figure 7 Spread tow glass fabrics supplied by Isola Group.

To assemble a laminated device using CF/CAG electrodes, the separator dictating the electrode separation (hence dominating the electrical power density), is essential to inhibit electrical shorting, but also the need to offer a tough ply interface and some mechanical stiffness. The separator materials selected for current and future device manufacture are shown in Figure 7 and Table 2. The 50 µm thick plain-weave E-glass fabric (Isola Group) has excellent mechanical properties. The 23 µm thick polyester/ceramic separator (Freudenburg) is easier to handle and better for preventing short-circuiting of devices.

Table 2 Specifications of polyester/ceramic separators selected for structural supercapacitor manufacture.

Material	Units	FS 3012-19	FS 3011-23	FS 3009-25
Material composition		Polyester/Ceramic	Polyester/Ceramic	Polyester/Ceramic
Thickness	[µm]	19	23	25
Area Weight	[g/m²]	29	33	35
Theoretical Porosity	[%]	53	55	55
Gurley Value (100ml)	[s]	70	110	100
Tensile Strength (md)	MPa	17	27	33
Tensile Strength (cd)	MPa	6.4	11	12

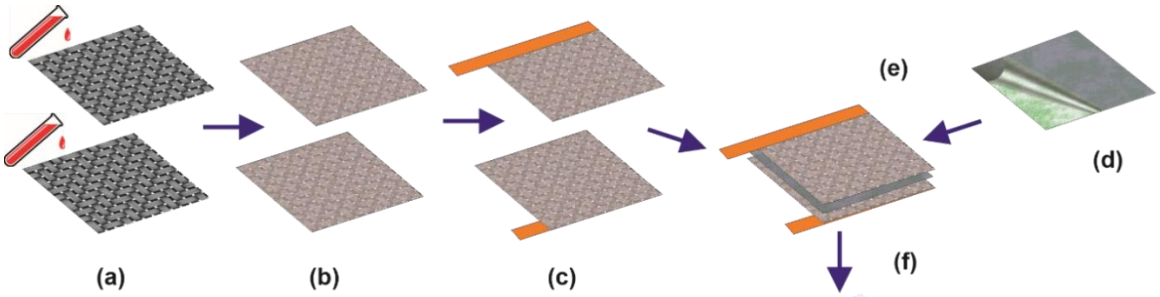

(a) Infuse individual CF lamina with CAG precursor and then age;
(b) Pyrolyse individual lamina to form the CF/CAG;
(c) Attach current collectors;
(d) Prepreg separator with multifunctional matrix;
(e) Assemble device to produce CF/Sep/CF laminate;
(f) Infuse laminate with liquid electrolyte;
(g) Encapsulate device in insulating, structural composite.

Figure 8 Fabrication process for the structural supercapacitors.

The manufacture process of the multifunctional device is shown in Figure 8. Firstly, CF/CAG lamina were prepared: carbon fibre fabrics were treated with a precursor (Figure 8a) using a resin infusion flexible tooling (RIFT) process and pyrolysed (Figure 8b). Current collectors were then attached (Figure 8c), following which the separator was prepregged using the structural electrolyte (Figure 8d). The separator was then sandwiched between two CAG-modified carbon fibre fabric electrodes (Figure 8e), the device was cured and then backfilled with additional ionic liquid (Figure 8f). Finally, the device was encapsulated to isolate from the environment (Figure 8f).

Figure 9 shows the morphology of the glass fibre separator layer in a cured composite device (Figure 8e) after being peeled apart (mode-I delamination). A regular pattern of structural electrolyte had formed between the glass fibre fabrics and CAG-modified carbon fibre fabrics, which can transfer load throughout the composite device.

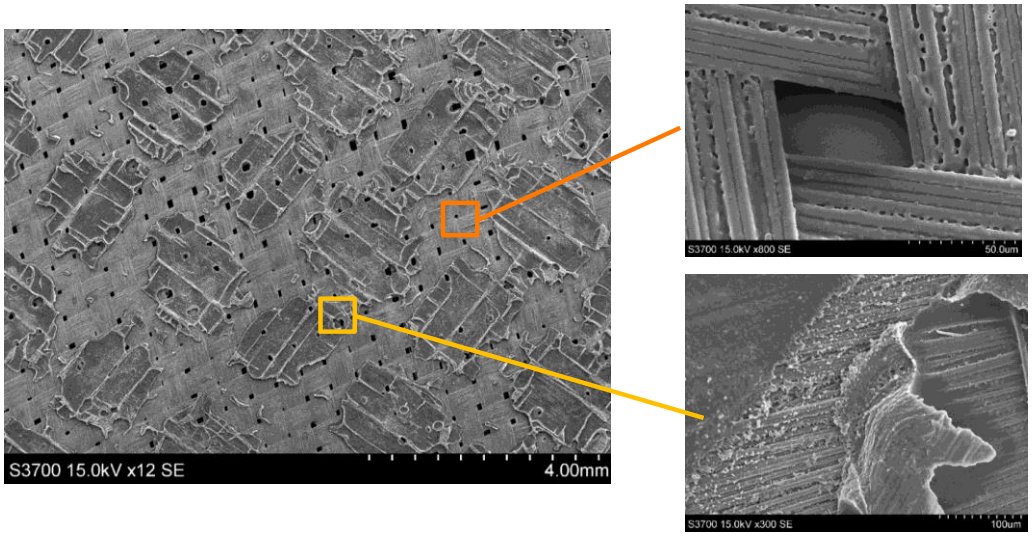

Figure 9 Electron micrographs of the CF-CAG/multifunctional matrix interface showing the differences in the thickness of resin film layers in various regions of the device.

Table 3 Summary of semi-structural (italics) and structural device performance with different separators with Textreme CF-CAG 43 gsm electrodes.

Electrodes	Separator	Electrolyte	C (F)	m (g)	V (V)	ESR (Ω)	C* (F/g)	E* (Wh/kg)	P* (kW/kg)
CAG CF 43 gsm	Woven GF (242 µm)	EMI-TFSI	0.68	0.91	2.7	2.66	0.75	0.76	0.76
CAG CF 43 gsm	PET/ceramic (23 µm)	EMI-TFSI	1.00	0.36	2.7	1.49	2.8	2.8	3.4
CAG CF 43 gsm	Woven GF (50 µm)	EMI-TFSI/ epoxy	0.50	0.39	2.7	7.5	1.3	1.3	0.62
CAG CF 43 gsm	PET/ceramic (23 µm)	EMI-TFSI/ epoxy	0.50	0.36	2.7	4.8	1.4	1.4	1.1

To characterise the cell performance, devices were assembled, consisting of two electrodes (4 cm x 4 cm) separated by a separator and soaked in ionic liquid (EMI-TFSI). Graphite current collectors and contact tabs were used to introduce the current. These were then sealed in polymer bags to contain the liquid electrolyte. These are semi-structural devices since there was no structural matrix constituent. Studies were undertaken with two separator configurations; either using plain woven glass (242 micron thickness) or PET/ceramic veils (23 microns thick). The resulting specific device performance was characterised, by considering the masses of the two electrodes, separator and electrolyte, as shown in Table 3. Although both devices presented a similar capacitance, the lower mass (and thickness) of the PET/ceramic separator led to a superior specific energy and power storage (2.8 Wh/kg and 3.4 kW/kg) respectively.

Preliminary structural devices have been manufactured, in which the separator has been filmed with a multifunctional matrix that has been developed at Durham University [18]. Studies were undertaken with two separator configurations [17]; either using thin-ply woven glass (50 micron thickness) or the PET/ceramic veil (23 microns thick). As expected, this led to a drop in electrical performance, but is anticipated to provide a fully structural composite able to withstand matrix dominated loading conditions such as shear and compression. The semi-structural and structural devices made using the PET/ceramic veil were directly comparable, the latter presented a small drop in specific energy but a large drop in specific power with respect to the former.

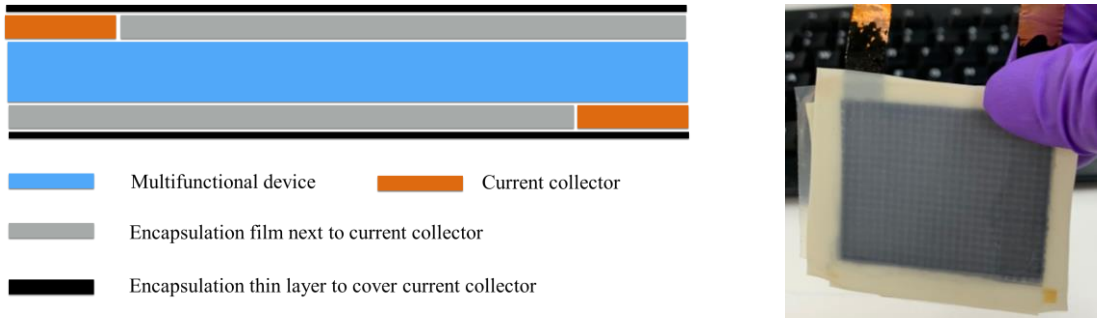

(a) (b)

Figure 10 (a) Schematics of the multifunctional supercapacitor encapsulated in structural polymer films (b) An example for multifunctional device after encapsulation

The laminated device prepared was a full cell flooded with ionic liquid electrolyte. To realise its application in aircraft structures, the multifunctional devices are required to be hybridised with structural materials which could prevent electrolyte leaching out [7] and subsequently encapsulated in structural CFRP composites, which permits loads to be transferred to the devices. Electrical collectors should extend from the electrode surface to the exterior of the encapsulated multifunctional structure for charging/discharging. PET and EVA were chosen from a review of insulating polymers, which could separate the device from the surrounding exterior and CFRP structural composites. Both were incompatible with the ionic liquid electrolyte and did not adsorb any electrolyte into the polymer, suggesting the potential to be used as a suitable encapsulation film for structural supercapacitors. Figure 10a shows a schematic of multifunctional supercapacitor encapsulated in polymer films. The copper tape current collector was passivated with carbon ink. As a result of ensuring even pressure on the electrodes, each electrode was applied onto an additional encapsulation film with the same thickness of the current collector, to fill in the gap between the outside encapsulation film and the electrodes without coverage of the current collector. An encapsulated device (Figure 10b) can be processed with carbon fibre prepreg in the autoclave. More encapsulation studies aiming at a combination of minimal power loss and maximal load transfer are still underway.

Device Characterisation

The effect of introducing CAG on the tensile and in-plane shear response was evaluated by ASTM standard coupon testing of four different hybrid laminates [19], all with plain weave glass fibre (GF) separators. Three configurations all used a structural epoxy matrix with (a) as-received CF (b) thermally-desized CF made using the same thermal cycle used for the CAG pyrolysis and (c) CF/CAG. The fourth laminate was the same as (c) but used a multifunctional matrix consisting of structural epoxy mixed with 40% by volume of EMIM-TFSI ionic liquid. The in-plane shear and Young's moduli were not affected by the CAG but varied when the multifunctional resin was introduced (Figure 11). The CF/CAG laminates, with both structural and multifunctional matrices, had tensile strength reductions of ca. 70% compared to the as-

received CF laminates, whereas the thermally-desized CF led to a 15% tensile strength reduction. One hypothesis is that this drop in tensile strength is associated with chemical reactions that occurred during the pyrolysis of the CAG, possibly those reactions that produce steam capable of degrading the carbon fibres. Another hypothesis is that the highly crimped nature of the plain weave fabric combined with the surrounding brittle CAG that enhances stress transfers between tows may be leading to this premature failure. Further investigation is underway to understand the main source of the tensile strength reduction and subsequently develop mitigation strategies.

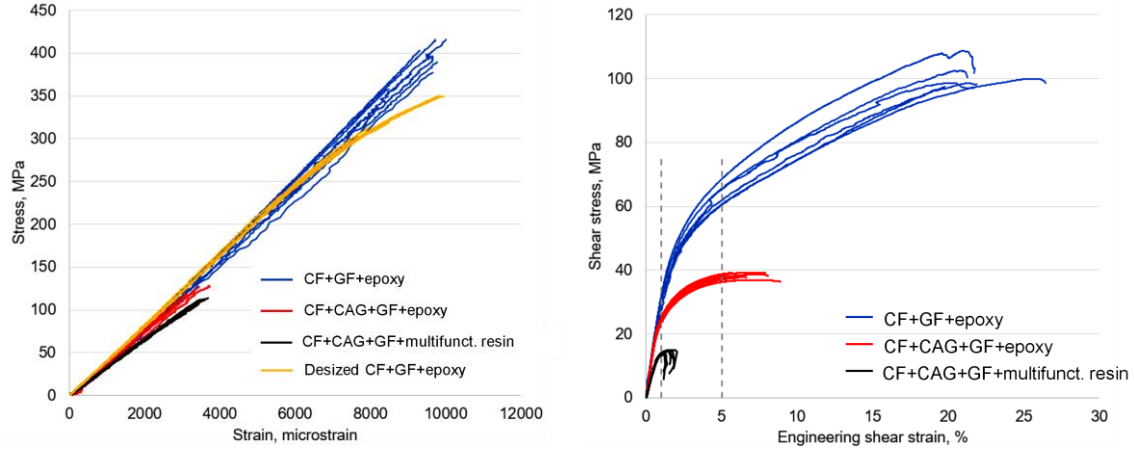

(a) (b)

Figure 11 Results from (a) longitudinal tension and (b) in-plane shear testing of standard coupons for monofunctional and multifunctional materials.

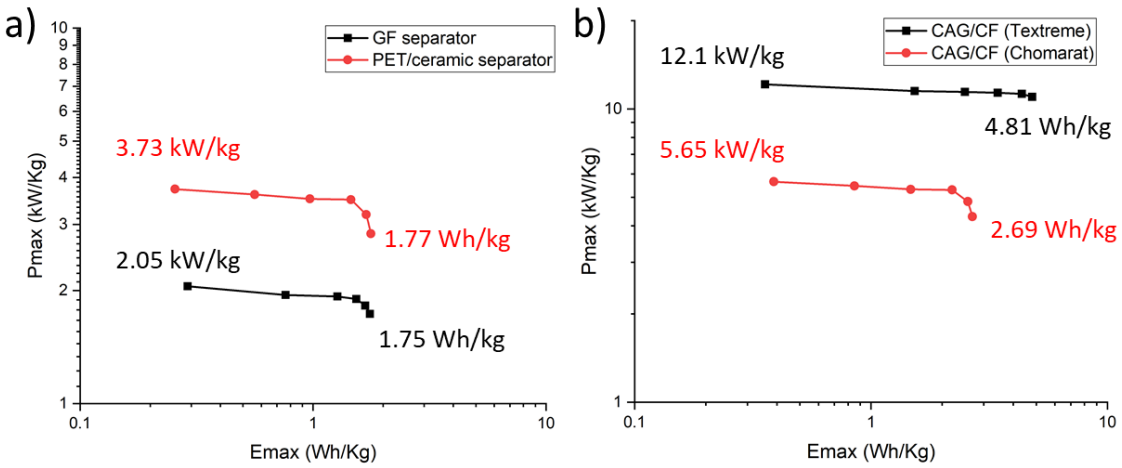

Figure 12 Swagelok cell test apparatus used to test 1 cm diameter structural supercapacitors and results of charge-discharge test for laminated devices with various (a) separators and (b) electrodes

To characterise the cell performance, devices were assembled in a two-electrode Swagelok cell consisting of two electrodes (diameter 1 cm) separated by a separator and soaked in ionic liquid (EMI-TFSI). The Swagelok cell setup was able to achieve test conditions resulting in > 80% of the maximum electrochemical capabilities of the device. The effect of the separator and CF fabric type on the electrochemical performance of supercapacitor were studied. The use of the thinner PET/ceramic separator (23 µm) led to an increase in the maximum power density as compared to the 50 µm thick woven glass fibre separator (Figure 12). A comparison between

the CAG-modified spread tow (Textreme, 43 gsm) and C-weave (Chomarat, 200 gsm) CF fabrics indicated superior electrochemical performance for the former in terms of both maximum specific energy and power.

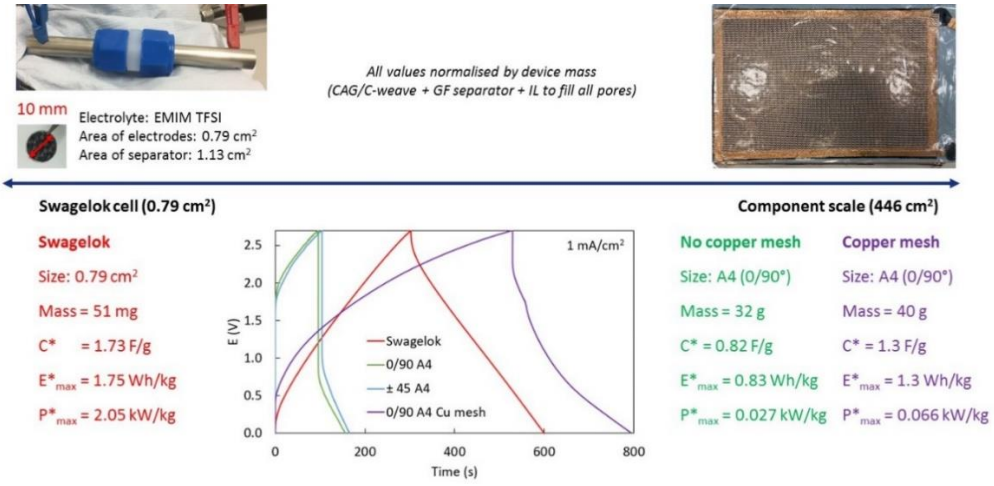

Figure 13 Electrochemical performance of < 1 cm² and A4 semi-structural supercapacitors with and without copper mesh.

An important part of the device assembly are the current collectors. Characterisation of the electrochemical performance of monofunctional and structural supercapacitors using 1 cm diameter Swagelok cell devices demonstrated that high specific energy and specific power can be achieved (Figure 13). However, upon scaling up the devices to 446 cm², the specific energy halved whilst the specific power dropped by two orders of magnitude. By using a copper mesh current collector, a specific energy of approximately three quarters of that in the Swagelok cell was measured. Although the specific power trebled, it remained well below that measured for the Swagelok cell.

The charge-discharge curves indicated high internal resistance losses without the copper mesh and significant resistance even with the copper mesh. A study was performed to quantify each ohmic resistance contribution (distinct from the ionic resistance in the electrolyte) to the overall internal resistance of the cell. Three sources of electrical resistance relating purely to the electrodes were identified: (a) the in-plane resistance through the electrodes; (b) the contact resistance between the electrode surface and the copper tape electrically connecting the electrodes to the electrochemical instrumentation; and (c) the through-thickness resistance between the exterior surfaces of the electrodes.

Experimental measurements to determine these three resistances [21] for single CF/CAG electrodes and thermally-desized CF fabrics were carried out using a four-wire digital multimeter with a Kelvin cable. For the same fibre orientations (0/90°), both with and without CAG, the spread tow fabric in-plane resistivity was just over twice that of the conventional plain weave (Figure 14). The different fibre types and presence of a binder in the spread tow are thought to have played a role. Additionally, the current flow in the direction between the connectors through the spread tow fabric is likely to be less uniform than for the traditional plain weave fabric. As expected, the in-plane resistivity was higher for fabrics at ±45° than at 0/90°. The introduction of CAG increased the in-plane resistivity for all fabrics tested, which may be attributed to cracks in the CAG preventing good electrical contact between the CF tows.

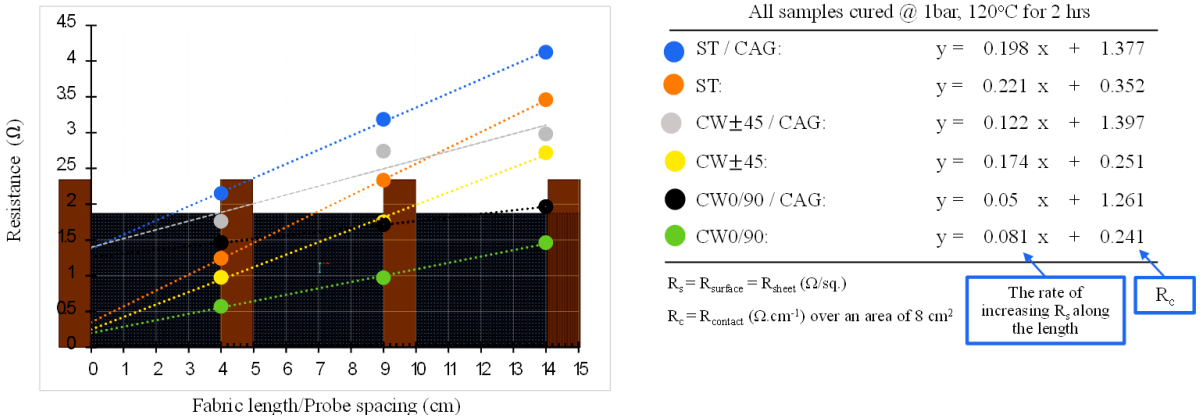

Figure 14 In-plane and contact resistances for plain weave and spread tow fabrics with and without CAG

For all fabrics tested, the contact resistance was at least four times higher when CAG was present, which may be attributed to cracks in the CF/CAG interface, as observed in polished cross-sections. These cracks are thought to have been introduced from CAG shrinkage during the cooling phase after pyrolysis, resulting in blocks of CAG that bowed away from the surface of the CF tows. This hypothesis was supported by electrical measurements performed at increasing levels of through-thickness compressive pressure. Increasing pressure led to reductions in contact resistance, suggesting that the CAG was making better contact with the CF tows. Further experiments are currently in progress to quantify the influence of compaction pressure more accurately during testing on all three electrical resistivity values.

Further evidence to support the hypothesis that CF/CAG interfacial gaps lower the conductivity was obtained by tests on thermally-desized CF fabrics without CAG and no pressure applied during testing. These thermally-desized samples yielded a contact resistance which was just under 25% of that measured using the as-received CF fabric without CAG and only 5% of the contact resistance for the CF/CAG fabric. This finding suggested that contact resistance in the final devices could be minimised by having current collectors directly in contact with the CF rather than the CAG. One approach to achieve this would be to mask predetermined regions or one surface of the fabric with an inert, removable substrate before infusing the CAG pre-cursor to leave some zones without CAG. After removing the substrate, the current collector would then be able to make intimate contact with the CF, thereby enabling good electrical contact without the need for high compaction pressures.

The tests mentioned above have also been carried out with other current collection materials including aluminium foil and grafoil strips. These latter two current collection materials gave equivalent in-plane resistances, as expected, but higher contact resistances than the copper tape since they did not have conductive adhesive to form a good electrical contact with the CF/CAG.

Multifunctional Modelling

A physics-based meso-scale finite element model (ABAQUS) was developed to investigate the mechanical and electrochemical behaviour of structural supercapacitors. The concept of multifunctionality requires that both design philosophy and predictive modelling tools advance beyond those currently used in conventional ‘monofunctional’ engineering fields. Multifunctional design is a multi-physics, multi-objective optimisation problem, and as such, it requires an integrated multi-physics modelling framework to support it. Current research aims to establish a multi-physics modelling methodology for structural supercapacitor composites. This work is building on mechanical models (ABAQUS) and electrochemical models (COMSOL, MATLAB). Further development and validation of this integrated

modelling framework (Figure 15) are underway.

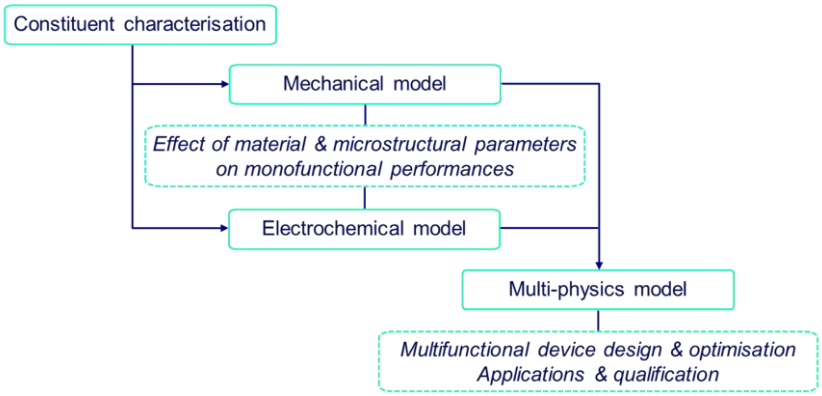

Figure 15 Integrated modelling framework to simultaneously predict the mechanical and electrochemical behaviour

It is expected that the electro-mechanical properties of hybrid composites are strongly dictated by the morphology of the compacted reinforcements, yet no investigations into their compressibility have been reported. A meso-scale modelling strategy was developed to investigate the effect of hybridisation and presence of CAG on the compaction response of multilayer stacks combining different dry woven fabrics [22]. Following established methodologies, finite element unit cell models were constructed from the average microstructural and compressibility properties of the constituent glass and carbon fabrics (Figure 16a).

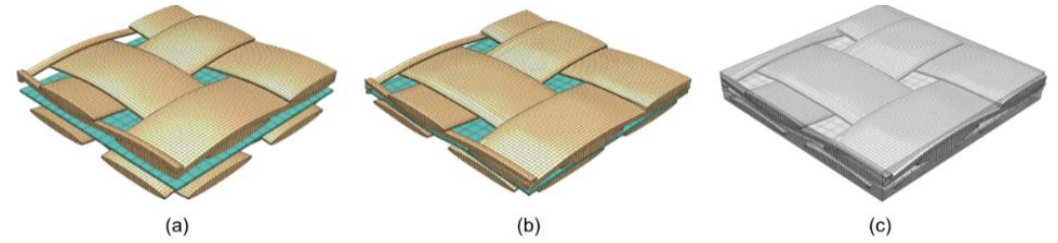

Figure 16 (a) Idealised reinforcement, (b) compacted reinforcement and (c) composite unit cell model of structural supercapacitors.

To represent realistic layups whilst maintaining high computational efficiency, several ply offset cases were considered. User subroutines for the non-linear elastic constitutive response of the reinforcements were developed. Model predictions were evaluated against compressibility measurements for monolithic and hybrid fabric stacks (Figure 17). The ply offset had a major influence on the predicted internal morphologies (Figure 16b) and fibre content, contributing to experimental variability. Optical microscopy (Figure 18) and micro X-ray computed tomography imaging further indicated greater likelihood of intermediate ply-offsets in physical specimens, over limit case idealisations. Compressibility was slightly reduced in the hybrid structural supercapacitor reinforcement stack compared to a conventional monolithic stack.

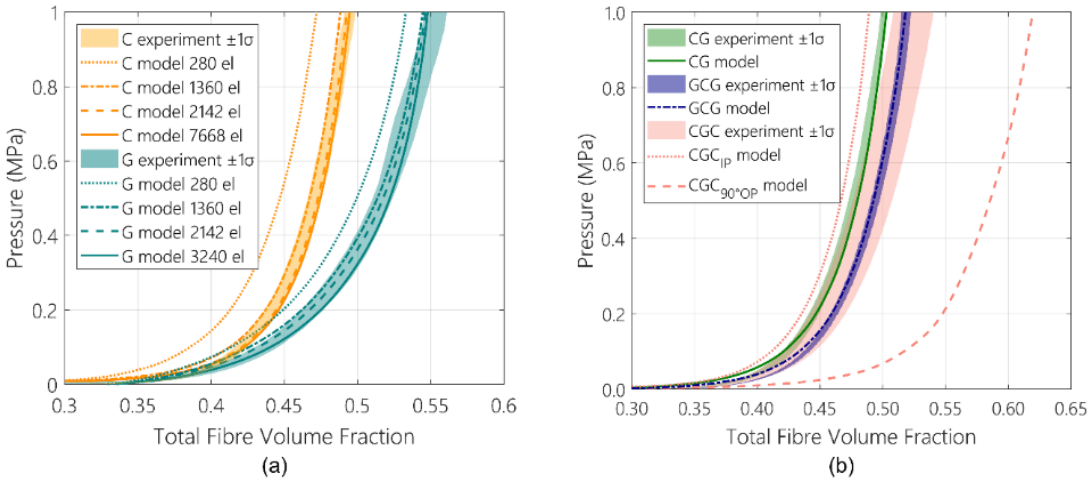

Figure 17 (a) Calibrated compressibility response of single carbon (C) and glass (G) fibre reinforcement plies, (b) comparison between experimental and predicted compressibility responses for hybrid multilayer reinforcement stacks.

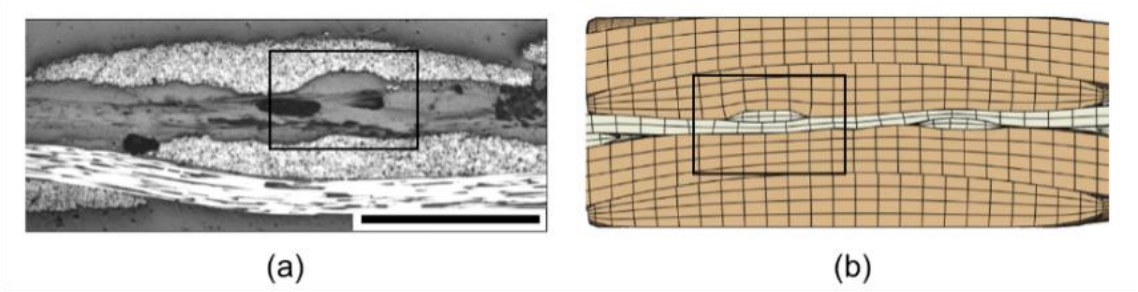

Figure 18 (a) Cross-sectional micrograph of structural supercapacitor composite, (b) dry reinforcement consolidation model.

The compaction models have been adopted to predict the final device meso-morphology and generate composite models (Figure 16c), enabling parametric investigations into various reinforcement and nano-reinforcement architectures, matrix formulations etc. Mechanical analyses to date have investigated the influence of carbon aerogel microstructure on the elastic response under tension and in-plane shear loading (Figure 19). The analysis suggested that significant improvements in the mechanical properties of carbon aerogel-modified laminates could be achieved through better control of the processing conditions.

Model validation is ongoing and has been facilitated by recently obtained experimental mechanical, digital image correlation and fractographic data from a comprehensive set of uniaxial tension and in-plane shear experiments for both structural power laminates and their monofunctional structural equivalents. The model is expected to provide insights into the effects of layup hybridisation, carbon aerogel modification and high matrix compliance on the composite elastic properties. The models developed can facilitate detailed damage initiation and progression analyses, including yarn-yarn and yarn-matrix cohesive zone interactions. This mechanical modelling forms a basis for the ongoing development of multi-physics models for multifunctional performance prediction and optimisation.

Finite element (FE) models focussing on the mechanical aspects [23] have been investigated to (a) reproduce the measured response of laminated structural supercapacitors, (b) capture tow nesting during compaction of the hybrid assembly of woven fabric plies, (c) undertake sensitivity studies to understand the main parameters influencing the mechanical properties and

(d) predict the performance of arbitrary device configurations.

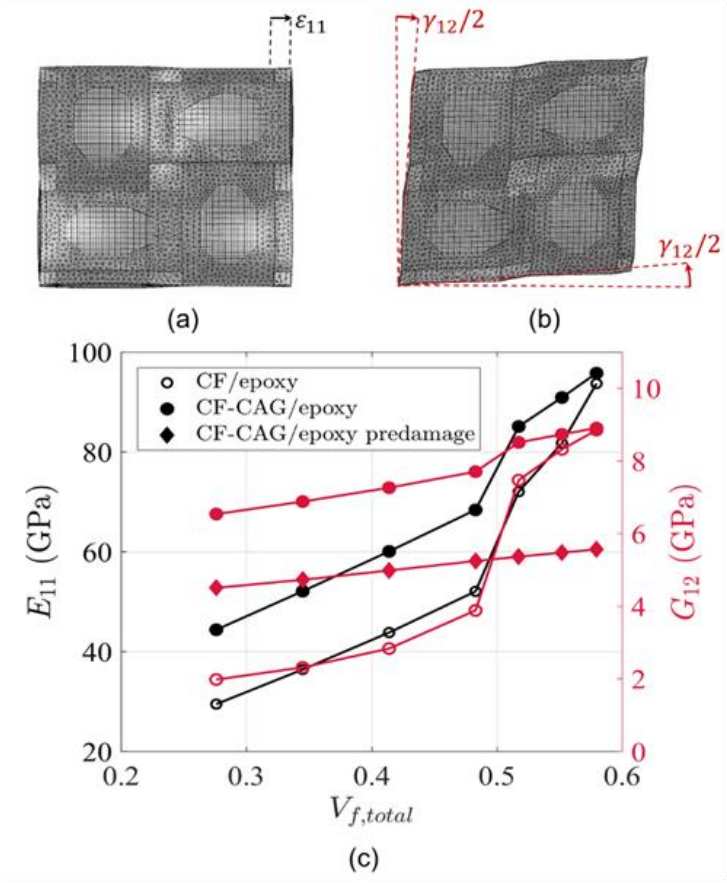

Figure 19 Electrode (CF) ply unit cell model with applied (a) tensile and (b) in-plane shear deformation, and (c) corresponding elastic response predictions with and without CAG

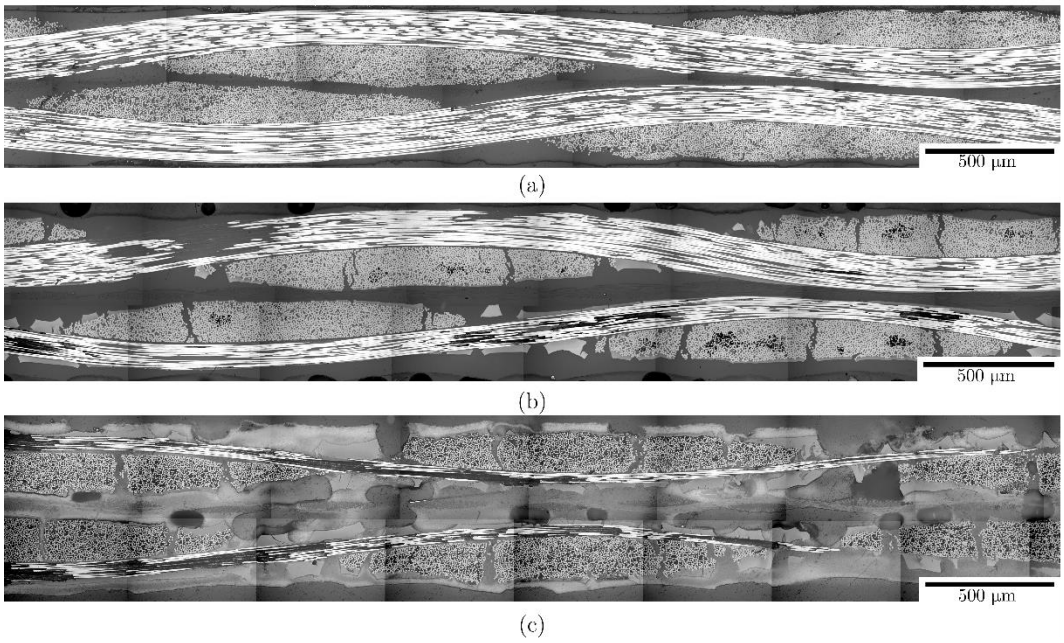

Figure 20 Optical micrographs showing the through the thickness architecture of the (a) Structural laminate without CAG; (b) Structural laminate with CAG and (c) Structural supercapacitor with CAG and structural electrolyte [23]

The starting point was a dry fabric compaction model followed by further refinements which are being supported by experimental validation. Tests to obtain material parameters for the models include dry fabric characterisation to measure longitudinal shear modulus, transverse modulus, initial inter-yarn fibre volume fraction, inter-yarn friction and the CF-CAG interface strength. Once these models have been verified, undergone mesh sensitivity studies and optimisation of the computational efficiency, a full composite model will be generated including resin pockets and voids to capture any manufacturing induced defects and understand their effects on the mechanical performance.

Cross-sections of CF/GF and CAG-CF/GF laminates (Figure 20) were examined to form a basis for the mesh geometry to be used in FE compaction models to determine the fibre volume fractions to be achieved for optimal mechanical performance.

The modelling approach selected was to use Abaqus/Explicit to develop a fully parametric, mesoscale fabric model with periodic unit cells (Figure 21). The tows are modelled using orthotropic continuum elements with geometric, material and contact non-linearity, including frictional sliding. The modelling procedure involved first defining an idealised fabric architecture from which to generate the woven fabric mesh. Since this process led to initial volumetric penetrations, these conflicts were resolved using an artificial thermal contraction and expansion step first excluding and then including contact. The fabric mesh is compacted between two rigid plates (Figure 22) until a target fibre volume fraction is attained, and the resulting geometry forms the basis for the generation of the composite architecture.

In-plane shear models (Figure 23) of the dry fabric and full composites were then created to predict the matrix-dominated mechanical properties, starting with the elastic mechanical properties followed by investigation of damage initiation and softening. These models were validated against ±45° tension tests.

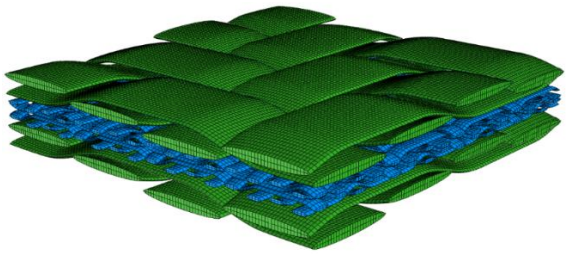

Figure 21 FE model of dry woven CF fabrics sandwiching a GF separator prior to compaction.

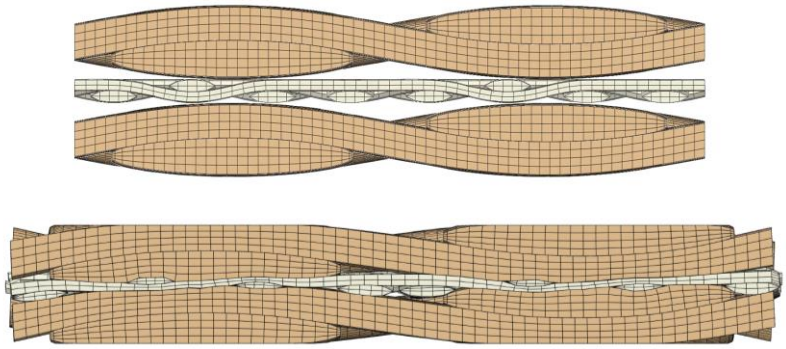

Figure 22 FE model of dry woven CF fabrics sandwiching a GF separator before and after compaction

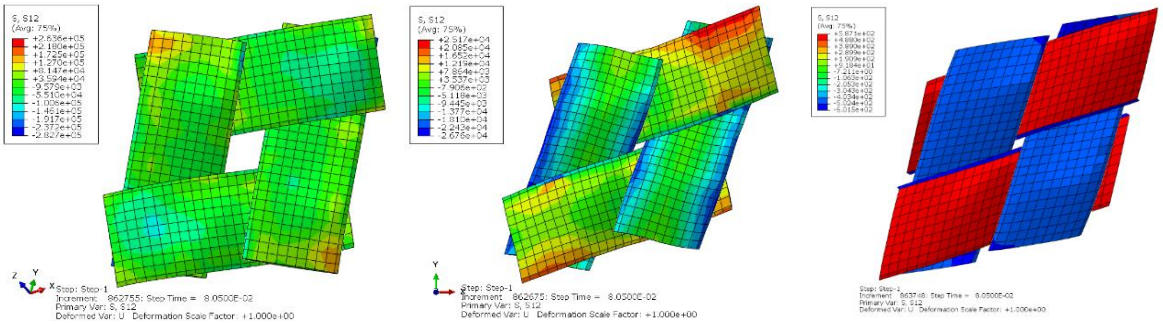

Figure 23 FE model showing the in-plane shear response of a dry woven carbon fabric

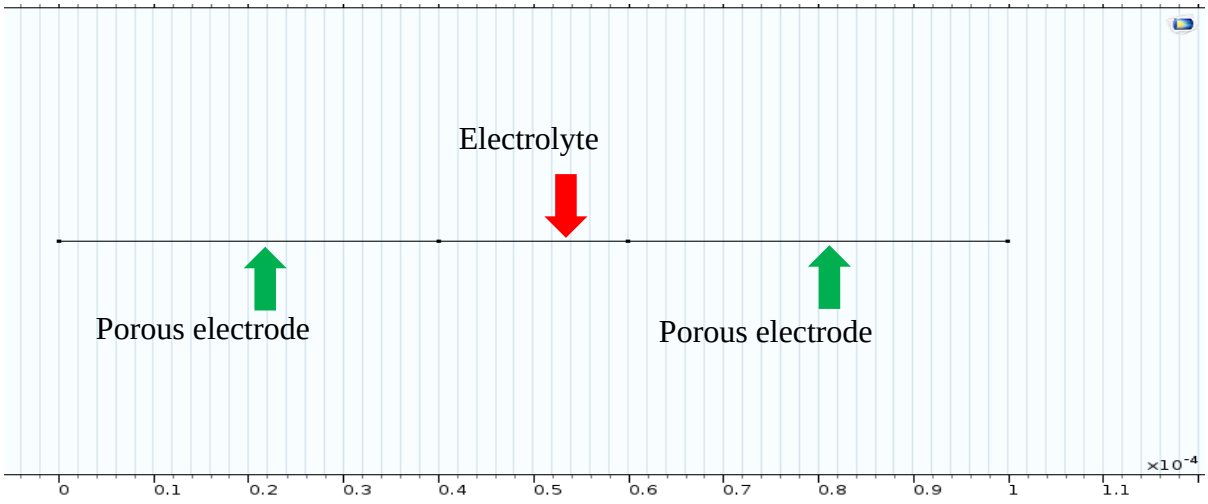

Figure 24 1D Comsol model of an electrolyte between two porous electrodes

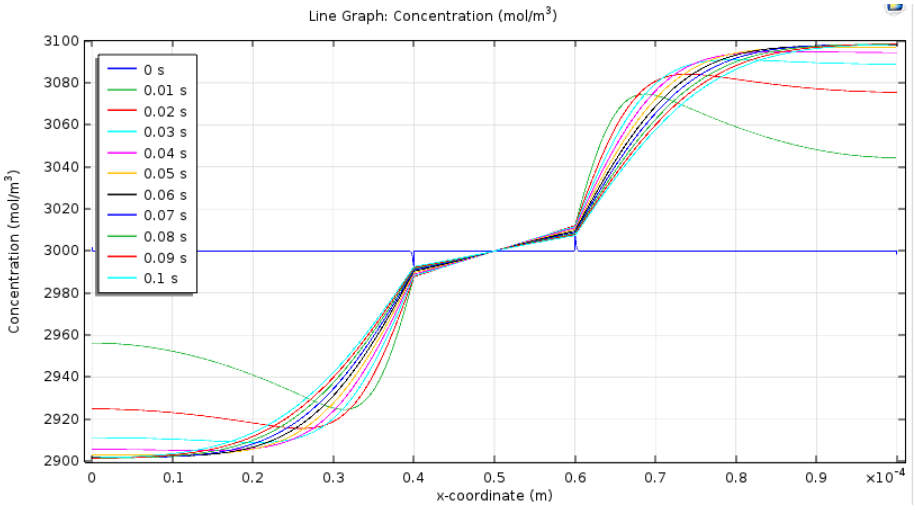

Figure 25 Cation concentration versus the through-thickness position of a structural supercapacitor

The development of electrochemical models [24] has aimed to (a) predict electrical performance based on constituent properties, (b) validate the models by comparison with the literature, and (c) understand the behaviour of real systems. The models will also facilitate

parametric studies into the critical parameters for structural supercapacitor design and optimisation. In the long term, these models will provide a framework to support qualification of structural power devices and by coupling the electrical and mechanical models, the overall multifunctional performance of a component can be optimised.

The approach taken has been to use the Comsol Multiphysics time-dependent solver with the following baseline parameters: ±0.05 V potential, 20 μm thick electrolyte (3 M KCl, diffusivity: D = 1.9 ×10-9 m²/s); 40 μm thick electrode (0.24 porosity); and CAG electrical conductivity: 5 S/cm. The parameters varied in the model include the electrode spacing, porosity and conductivities; electrolyte properties; separator porosity/tortuosity and pseudocapacitance. A schematic of the initial 1D model is shown in Figure 24, and the cation concentration as a function of the position through the thickness of the laminate are shown in Figure 25.

The 2D model was developed to incorporate the carbon fabrics and study the blocking effects introduced by the 7 μm diameter carbon fibres. It was assumed that the fibre volume fraction in the porous electrode was 60 % and the remainder of the volume was filled with CAG. Note that 60 % is the gross volume, since the electrolyte will need to infuse into the CAG. Only the minimum simulation domain required was considered (Figure 26 and Figure 27). The current 2D model has been shown to generate comparable capacitance results to that given in the literature.

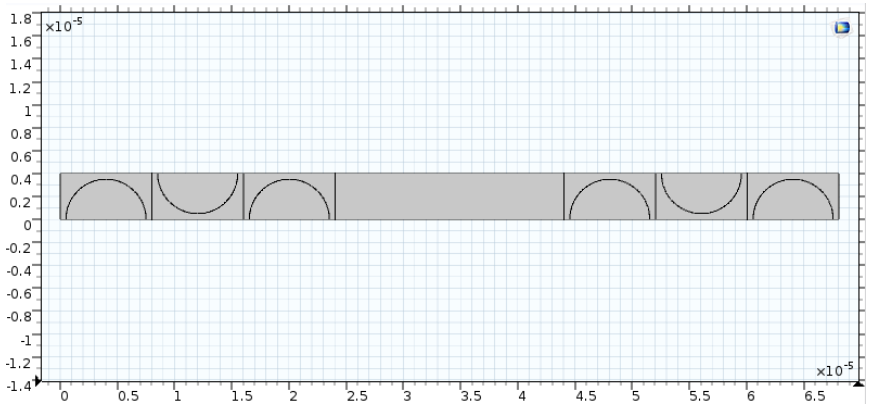

Figure 26 2D Comsol model of an electrolyte between two porous electrodes

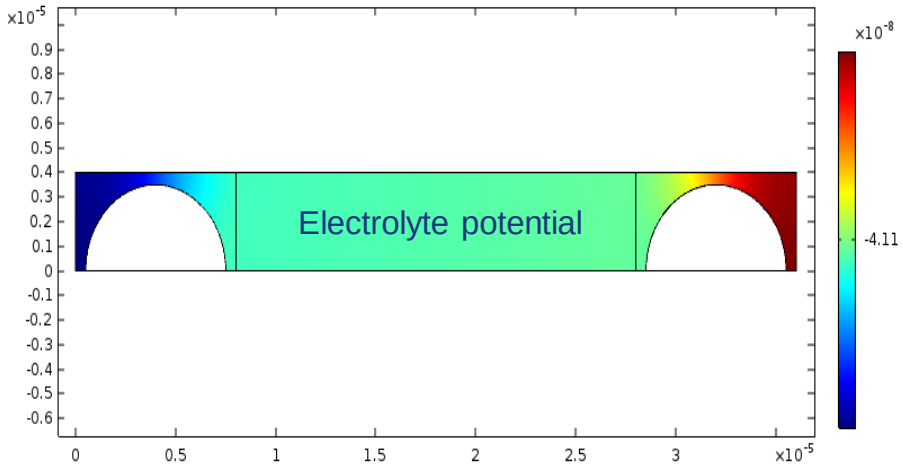

Figure 27 Electrolyte potential versus position within a structural supercapacitor

To understand the critical electrochemical parameters and optimise the design of structural supercapacitors, a 1D COMSOL model was developed involving the porous electrodes, separator and electrolyte. The main mechanism during charging and discharging is the

adsorption and desorption of ions on the porous electrodes. During charging cations flow towards the negative electrode, and anions to the positive electrode. Upon discharge, the directions are reversed. At the electrodes, an electrical double layer is formed comprising of a Stern layer and a diffuse layer.

Parametric studies investigated the effects of several parameters on supercapacitor performance. The main influencing factors are the electrode potential; the electrode and separator thicknesses and porosities; and the electrolyte diffusion coefficient and concentration. The supercapacitor performance was evaluated in terms of the specific capacitance, specific energy and specific power. The modelling entailed five main assumptions. Firstly, the device area was much larger than the device thickness, such that the cell could be considered one-dimensional. Secondly, the electrolyte was binary and symmetric, i.e. it contained only one type of cation and one anion and dissociated into equal numbers of anions and cations. Thirdly, the model adopted dilute electrolyte theory and assumed a homogeneous diffusivity throughout. Fourth, the double layer was thin compared to the pore size. Fifth, the model assumed negligible faradaic processes, i.e. the energy storage was purely via double layer charging.

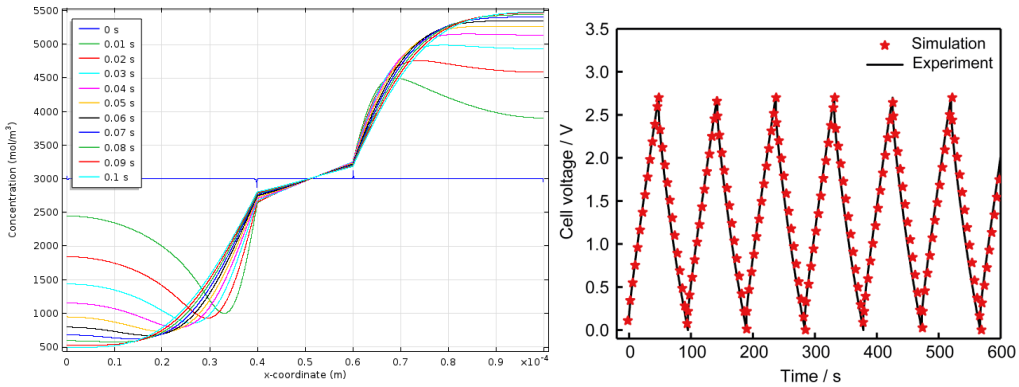

(a) (b)

Figure 28 (a) Spatial distribution of cations during charging (2 V cell, 24% electrode porosity) and (b) Galvanostatic charge-discharge of a semi-structural supercapacitor with CF/CAG electrodes and a GF veil separator in EMIM TFSI at 20 mA.

In these models, the cations accumulated in the negative electrode whilst being expelled from the positive electrode and the ion concentrations in the porous electrodes (Figure 28a) reached a steady state after approximately 0.1 s, for a 3 M binary (1:1) aqueous electrolyte. Corresponding experimental data for a semi-structural supercapacitor device showed good agreement with the simulated charge-discharge performance (Figure 28b). To study the effect of the electrolyte on the performance, electrolytes with a range of diffusion coefficients were modelled, covering the diffusivity of most aqueous and ionic liquid electrolytes used for energy storage. The electrolytes with high diffusion coefficients facilitated fast charging rates and therefore high specific powers.

Multifunctional Design

A challenge often encountered during conveying of multifunctional performance results presented using existing metrics is that to a lay audience without expertise in multifunctionality, multifunctional materials appear to have low performance compared to those of their monofunctional counterparts. For instance, using traditional metrics, a structural battery with a specific energy of 110 Wh/kg would be considered to have a performance marginally over half that of a conventional lithium ion battery (~200 Wh/kg). Similarly, the

specific power or specific Young's modulus of structural supercapacitors would both appear too low to merit consideration ahead of conventional materials and devices. This perception of low performance stems from not taking a holistic viewpoint. Presenting system-wide mass savings or showing multifunctional efficiency indices have been developed to capture the multifunctionality to some degree. However, to interpret and compare with familiar material properties, these approaches do not present the results in the way end-users would prefer to use them.

Instead, we have developed a new way to present multifunctional performance results, using 'residual specific' properties [25]. To demonstrate this methodology, residual specific properties were determined for two cases; a structural battery and a structural supercapacitor. Performance data from previously published models [**Error! Reference source not found.**] was used to determine a structural battery with the same global bending stiffness of a conventional composite panel to have a residual specific energy of 409 Wh/kg. Similarly, this method was applied to structural supercapacitors and yielded a residual specific power of 4.33 kW/kg which slightly exceeded that of a comparable size commercial off-the-shelf (COTS) supercapacitor (Figure 29). This research also highlighted an important recommendation for the multifunctional material research community: comparative monofunctional data should be presented alongside multifunctional material data to enable fair and accurate evaluations that facilitate optimal system design.

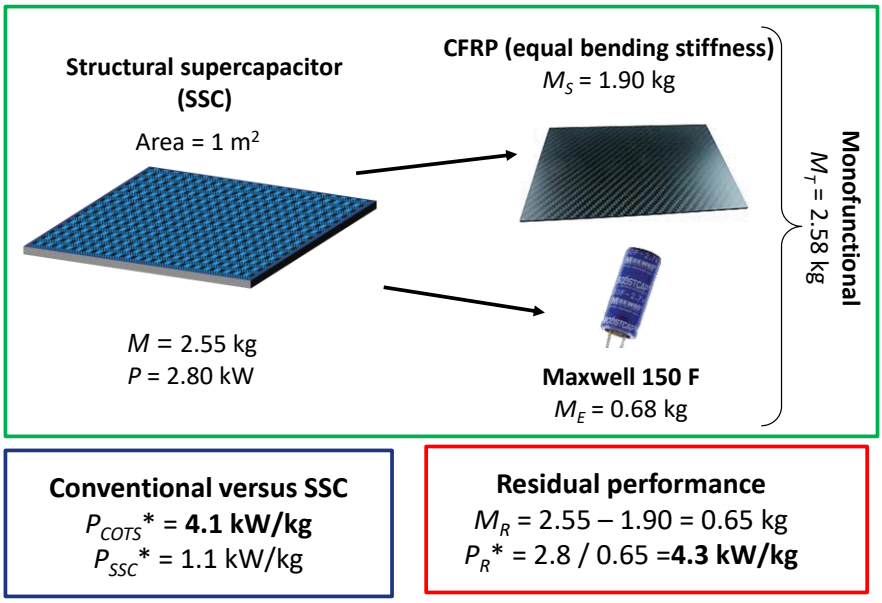

Figure 29 Application of the residual performance methodology to structural supercapacitors

A theoretical investigation was carried out to consider the potential use of structural power composites in regional aircraft passenger cabins [26] and the corresponding challenges to widespread use, including fire resistance, long-term cycling performance, and cost. This study focused on adapting sandwich floor panels with structural power composite face sheets, designed to power the in-flight entertainment system. This investigation selected a widely-used aircraft (A220-100) as a case study to demonstrate the methodology and determines the mechanical, specific energy and specific power requirements, as well as the mass, volume and emissions savings achievable. The proposed multifunctional design methodology consisted of five main stages: (1) Define performance requirements to determine the feasibility of using

multifunctional materials. (2) Explore how best to integrate multifunctional materials into new systems, configurations or architectures. (3) Select a multifunctional system configuration using a simplified analysis based on requirements for the proposed application. (4) Understand how integrating a multifunctional material affects the design of the associated mechanical and electrical systems. (5) Evaluate the benefits and challenges of using multifunctional materials for a given application.

Using a simple mechanical model to define the structural requirements, based on state-of-the-art laminated structural power composites, a series of electrochemical energy storage performance targets were calculated. For an Airbus A220-100, the analysis predicted potential mass and volume savings of approximately 260 kg and 510 litres and annual reductions in CO_2 and NO_x emissions per aircraft of approximately 280 tonnes and 1.2 tonnes, respectively, provided the structural power composite can achieve the following properties: specific energy > 144 Wh/kg, specific power > 0.29 kW/kg, in-plane elastic modulus > 28 GPa and in-plane tensile and compressive strengths > 219 MPa. These performance targets can help researchers developing structural power composites by guiding the selection and optimisation of the material constituents and fabrication processes. Significantly, the use of a distributed energy storage system offered a significant range of other mass and cost savings, associated with a simplified electrical distribution system design, and the use of ground-generated electrical energy. This extended design analysis of a specific component highlighted both the far-reaching implications of implementing structural power materials and the potential extensive systemic benefits.

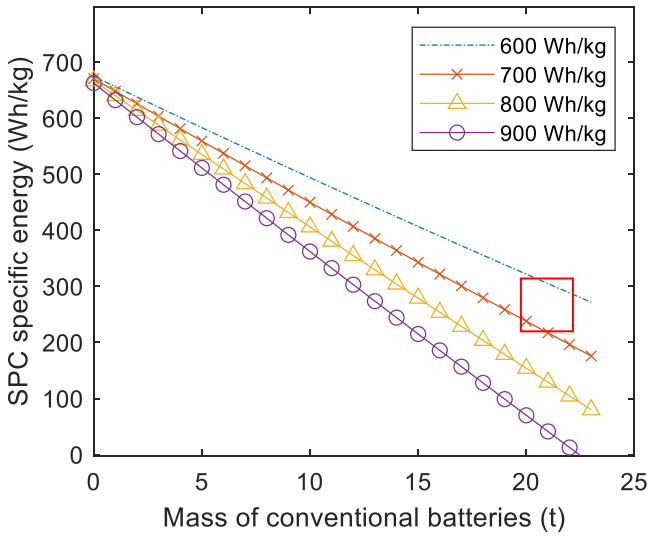

Figure 30 Structural power composite performance requirements for a 1000 km range all-electric A320 with strut-braced wings with different monofunctional battery (pack level) specific energies. The red box highlights a zone which requires relatively modest monofunctional and structural battery specific energies.

The future of commercial aviation is driven by the need to improve efficiency and lower emissions. All-electric aircraft present a route to eliminating direct fuel burn emissions, but their development is stifled by the limitations of current battery energy and power densities. Hence, another multifunctional design study investigated the feasibility of integrating structural power composites into future electric aircraft [27] and assessed the potential impact on greenhouse gas emissions up to 2050. Using the Airbus A320 as a platform, three different

electric aircraft configurations were conceptually designed incorporating structural power composites, slender wings and distributed propulsion. The specific energy and power required for the structural power composites were estimated by determining the aircraft mission performance requirements and weight. Compared to a conventional A320, a parallel hybrid-electric A320 with structural power composites (> 200 Wh/kg) could potentially increase fuel efficiency by 15% for a 1500 km mission. For a battery-powered A320, structural power composites (> 300 Wh/kg) could nearly halve the specific energy or mass of the batteries needed to power a 1000 km flight (Figure 30). Structural power composites could supplement or offer an alternative to higher energy density batteries and potentially enable lighter and safer electric aircraft.

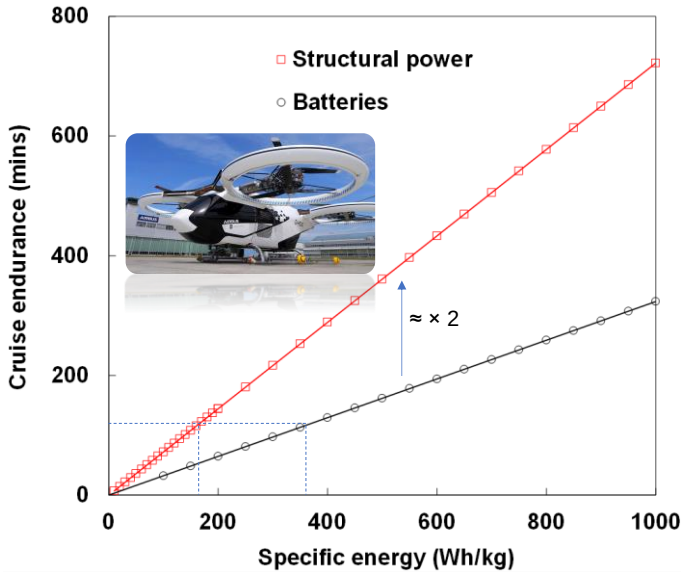

Figure 31 Cruise endurance for the CityAirbus powered by either monofunctional batteries or structural power of a given specific energy

The evolving field of urban air travel is leading the aviation sector towards a more sustainable future, driven by electric vertical take-off and landing (e-VTOL) aircraft with new technologies and electric propulsion systems. A multifunctional design study investigated the viability of using SPCs to supplement or replace monofunctional batteries within air taxis [28], specifically, the CityAirbus, a four-seater eVTOL currently under development. A typical mission profile was developed and used to determine the power and energy requirements for each flight segment. The mass of structural composites eligible for substitution with SPC was determined by a weight audit. Various scenarios with different take off masses and SPC masses were considered to determine the SPC target performance values to meet the needs of the CityAirbus mission profile. These targets were compared to those for monofunctional batteries (Figure 31). The target values for the mechanical requirements of the SPC were also determined based on the critical loading case likely to be experienced by the CityAirbus. Reduced SPC mechanical properties relative to conventional structural composites were considered for bending and in-plane loading to determine target values associated with increased thicknesses needed to carry the loads.

If all the eligible composite mass were to be replaced by SPCs, the mass of the CityAirbus could be reduced by 23%, since the batteries and 60% of its associated wiring mass could be made redundant. The minimum specific energy and power requirements for the SPC were 53

Wh/kg and 140 W/kg, respectively. Furthermore, approximately 55% endurance gains could be achieved by replacing monofunctional batteries with SPC at the same specific energy. This study into SPC applications in the CityAirbus indicated that the urban air transport sector presents a promising adoption route for SPC technology. Furthermore, SPC has the potential to aid in progressing the commercialisation of air taxis by making the range more attractive to potential customers or allowing greater payloads to be carried by removing monofunctional batteries.

Demonstration

Part of the work undertaken was to demonstrate the use of structural power materials to replace a fuselage C-section spar (Figure 32a) in the Airbus A350 and a bank of conventional Maxwell 150 F supercapacitors (Figure 32b) located on the door (Figure 32c). The supercapacitors weigh approximately 60 kg and provide 130 W to produce the torque to open the door in an emergency. Tooling for the C-section beam (Figure 32d) had been received from DLR and has dimensions 120 × 14.5 × 7 cm^3. The tool has been successfully used with low temperature cure carbon fibre fabric prepreg for trial manufacturing of a monofunctional C-section beam (Figure 32e). The demonstrator (Figure 32d) was to be a representative element which is multifunctional in the web region (blue) rather than the whole fuselage beam.

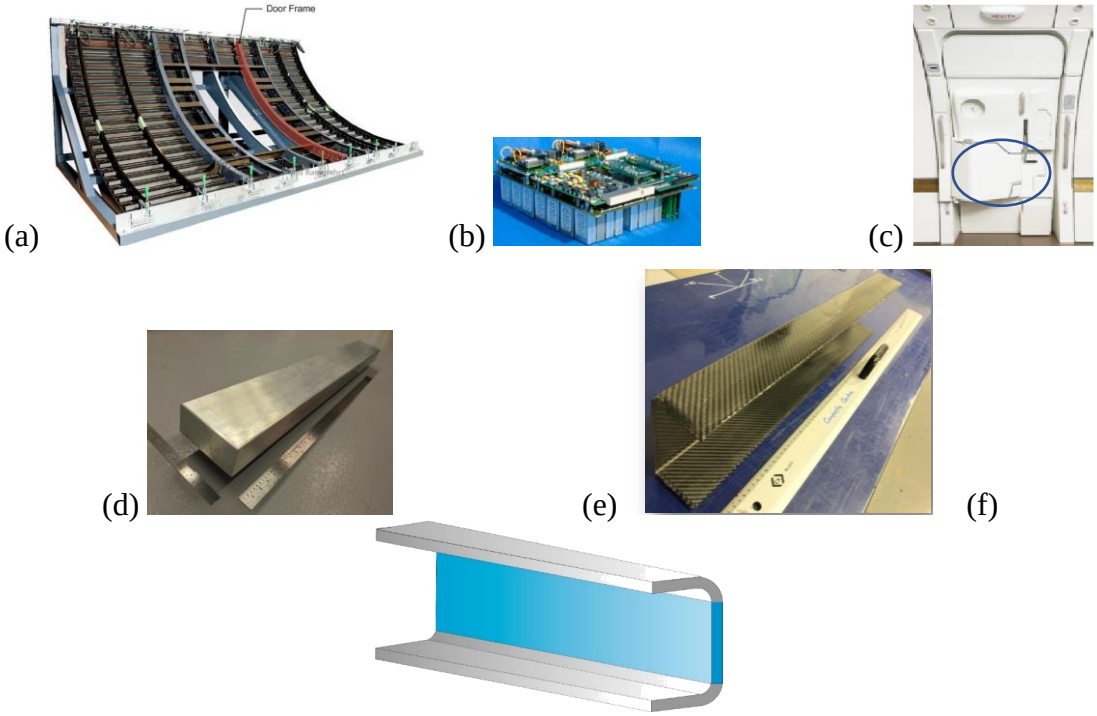

Figure 32 Location of the actual curved door frame shown in red (b) supercapacitor bank and circuit board (c) passenger door showing the location of the supercapacitor bank circled (d) Stiffener tool from DLR (e) manufacturing trial to produce a monofunctional C-section beam (f) proposed multifunctional web of the C-section beam

The potential mass saving if SPC is used to power all sixteen passenger doors is approximately equal to the mass of sixteen supercapacitor banks totalling 67.2 kg. The potential volume saving if SPC is used for all doors could reach the volume of sixteen supercapacitor banks (0.21 m^3). Both of these benefits are conditional on the SPC being able to completely fulfil both the structural and power requirements provided by the existing C-frame beams and conventional supercapacitor bank without significant changes in mass or volume compared to the original beams.

The dimensions of the cells were limited by the web section width and the internal dimensions of the furnace chamber used for CAG manufacture (30 × 30 cm²). Each cell was designed to have individual encapsulation and the connections would be made such that any cells that had developed faults could be bypassed. This encapsulation will form insulating layers between individual cells and the external carbon fibre fabric plies to isolate the cells from the external environment. The final agreed target voltage for the demonstrator device was 6 V and therefore several supercapacitors needed to be connected in series. The number of supercapacitors required was determined by the nominal voltage of each cell. In the case of 2 V cells, stacks of three supercapacitors in series would be needed, with the number of stacks determined by the energy and power requirements. The proposed geometrical configuration was twelve cells (Figure 33) within the web section arranged in two adjacent stacks of six cells connected in series. In terms of the electrical connections, the cells would be connected to form four parallel-connected triple cells. Each cell has areal dimensions of 28 cm (length) × 11 cm (width). The total thickness of the layup (Figure 33) was estimated to be 3.4 mm, including external plies of low temperature cure tooling prepreg. Further details of all the materials in the demonstrator are shown in Table 5 and Figure 34.

Table 4 Specifications of all materials in the structural supercapacitor demonstrator

Function	Material	Plies	L (cm)	W (cm)	t (µm)	T (mm)	A (m^2)	ρ (g/ml)	ρ_A (gsm)	Mass (g)	Mass (%)	Vol (ml)	Notes
Structural CFRP	LT cure prepreg	11	60	29	250	2.8	1.1	1.6	400	439	55	275	2 x 2 twill weave
Encapsulation	Metallised polymer	24	30	13	75	0.9	0.9	2.0	150	140	18	70	PET-Al-PE-coating
Electrodes	Textreme CF-CAG	24	28	11	110	1.3	0.7	1.8	100	74	9	81	Web only, 0/90
Current collector	Al tape	24	28	5	70	0.8	0.3	2.0	142	48	6	12	Wurth Electronik
Electrolyte	Ionic liquid	24	28	11	80	1.0	0.4	1.5	121	45	6	30	EMIM-TFSI
Adhesive	Double-sided tape	14	30	7	40	0.3	0.3	1.3	52	15	2	12	10 mm wide strips, AT395
Separator	Polyester-ceramic	12	30	13	23	0.1	0.5	1.4	33	15	2	11	Freudenberg
External connectors	Al tape (extended)	24	38	1	70	0.4	0.1	2.0	142	13	2	3	5 cm excess length
Matrix	Epoxy droplets	24	28	11	20	0.2	0.4	1.3	25	9	1	7	BADGE + IPDA
Seal connectors	Hot melt adhesive	24	2	0.8	100	2.4	0.0	1.3	130	0	0	0	Pi-Kem, 55-75% EVA
						3.4				**799**		**500**	t = ply thickness

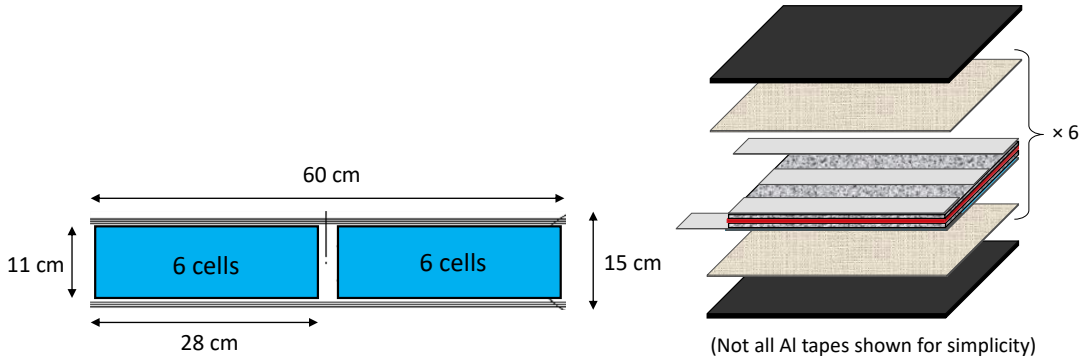

Figure 33 Configuration of the cells in the web section of the demonstrator beam

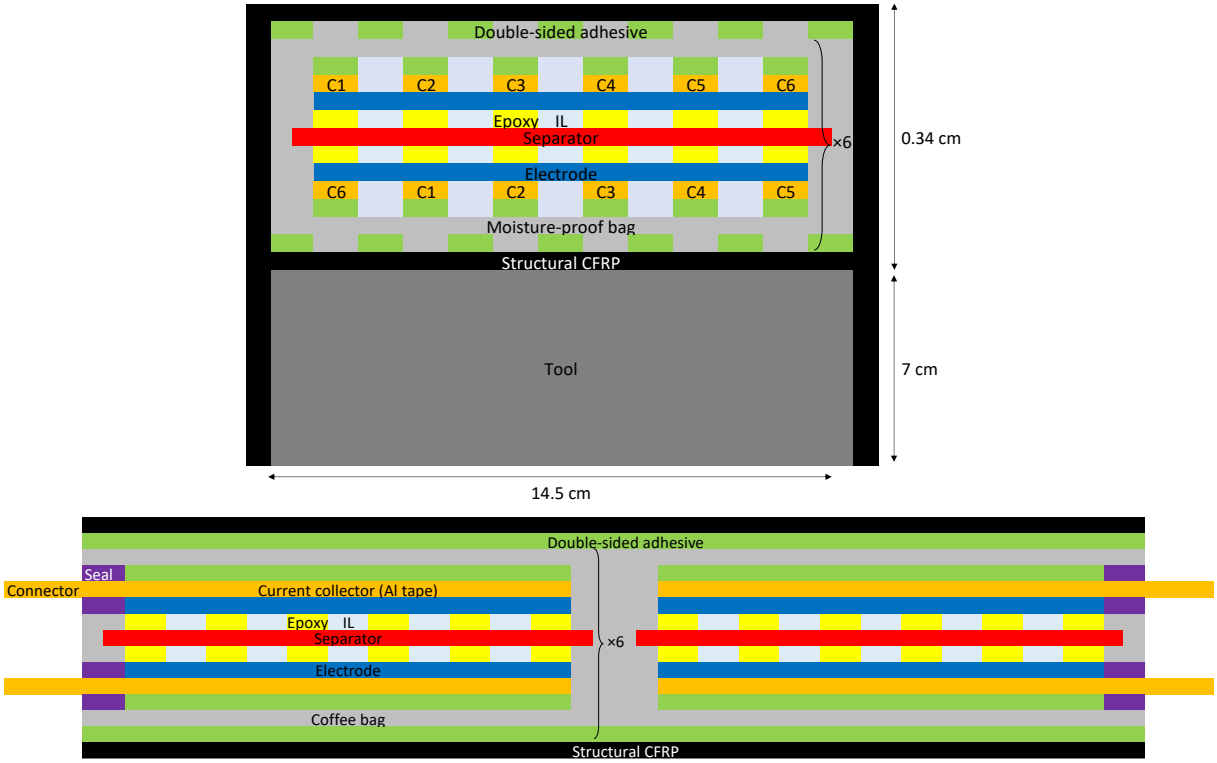

Figure 34 Cross-sections of the layup showing all the plies for only one cell per stack within structural CFRP plies.

A CAD model (Figure 35) of an aircraft fuselage and passenger door assembly was designed, (approximately A3 size), to demonstrate the multifunctional C-beam powering the aircraft door mechanism in an emergency situation. The majority of the parts were 3D printed using ABS and the fuselage and door were made from the same low temperature cure prepreg as the C-beam outer skins. The three detachable base parts serve both as a mounting point for the whole assembly as well as a supporting fixture to hold the structure on the ground; all other components were adhered by a structural toughened epoxy adhesive. The mounting angle of the fuselage skin was designed such that the door would open via a purely horizontal motion and therefore require minimal torque.

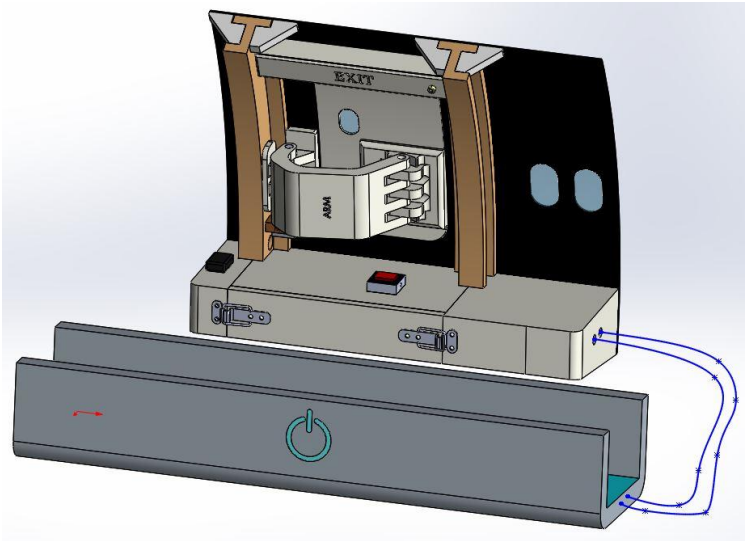

Figure 35 CAD model showing the scaled fuselage door assembly and multifunctional C-section beam (60 cm long)

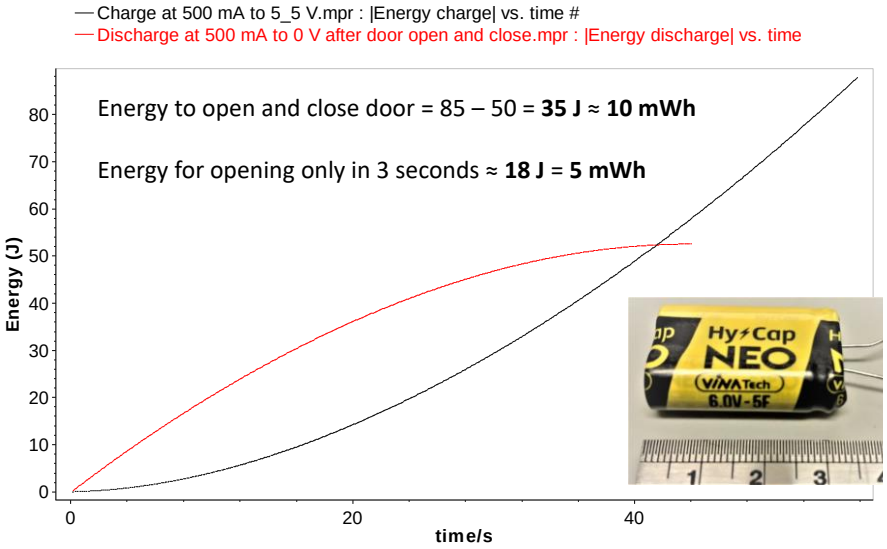

Figure 36 Energy consumption measurements for a commercial supercapacitor to open and close the demonstrator fuselage door.

The door opening mechanism was driven by a servo motor having an operating angle between 0 to 90° and operating voltages and currents of 4 - 6 V and 0.5 - 1.3 A, respectively. Experiments were performed to characterize the electrical power and energy required to open and close the scaled fuselage door with a 3 s opening time. A Biologic SP-240 potentiostat was used to charge a HyCap Neo 5 F commercial supercapacitor to 5.5 V at a constant current of 0.5 A (Figure 36). The supercapacitor was then connected to the servo motor and the door was made to open and close. The supercapacitor was then discharged at 0.5 A to 0 V using the potentiostat. An energy of 85 J was stored in the supercapacitor, of which 35 J (≈ 10 mWh) was consumed to open and close the scaled aircraft door. The average power and current were then calculated to be approximately 6 W and 1.1 A. These requirements were used to guide the series and parallel connections between the cells. For example, using four triple-cell stacks of structural supercapacitors connected in parallel, the current density per stack was calculated to be approximately 1 mA/cm².

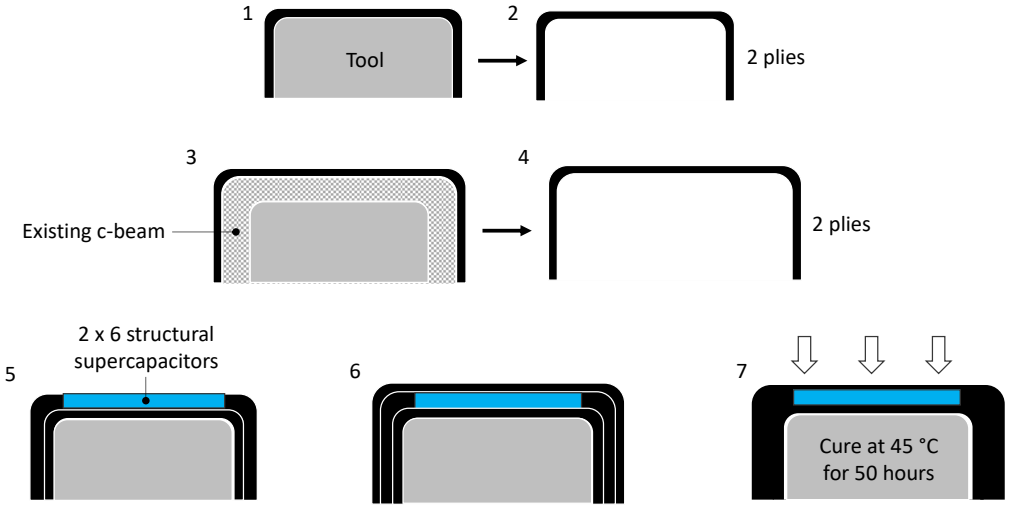

Figure 37 Main steps in the manufacturing process of the multifunctional C-section stiffener.

(a) 

(b) 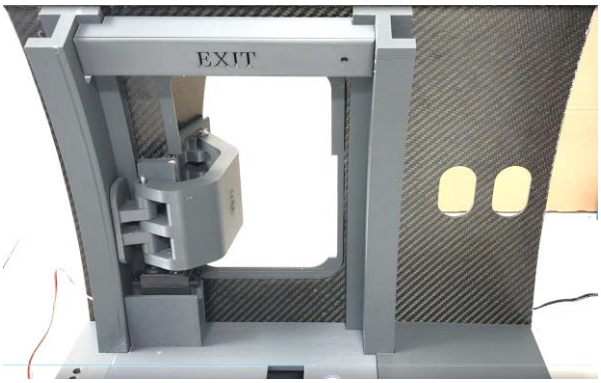


(c)

Figure 38 Scaled fuselage door assembly (a) inside view with the door closed (b) inside view with the door open (c) outside view.

In manufacturing scale-up trials, cells were made having half the area of the final demonstrator cell size. The half-size trial cell was measured to have a discharge capacitance and energy of 4.7 F and 3.4 mWh at a constant current density of 1.25 mA/cm². Although only the 4-6 V range of the structural supercapacitor stacks would operate the motor, this result nevertheless indicated that twelve full-size cells should exceed the required 10 mWh and 6 W. The extra power output could light three to four light emitting diodes (LEDs, 1.5 V, 20 mA) connected in series behind an "EXIT" sign above the door.

The method for manufacturing the multifunctional C-section beam are detailed below. At the time of reporting, the manufacturing was not completed because of delays from COVID-related lab access restrictions and variability in the electrode electrochemical performance. The manufacturing of the parts for the scaled fuselage door assembly has been completed (Figure 38) and the door mechanism was tested successfully.

The manufacturing process for the C-section beam involved the following steps (Figure 37):

- Insert device into PE/Al/PET bag with connectors protruding out;
- Infuse with EMIM-TFSI ionic liquid electrolyte under vacuum (> 12 h);
- Seal around connectors using holt melt sealing tape;
- Electrochemically test all devices using impedance spectroscopy;
- Assemble two stacks of six encapsulated devices on inner skin;
- Allow twelve Al tapes to protrude from each end of the beam;
- Electrochemically test all devices using impedance spectroscopy;

- Cut eighteen 0/90 plies of 60 cm × 7 cm low temperature cure prepreg;
- Lay up nine plies in each of the cap regions;
- Place outer skin over assembled stacks;
- Apply pressure and cure inner skin at 45 °C for 48 h.

It is anticipated that the demonstrator will be completed in the next few months.

Summary of Papers

Invited and Keynote lectures:

1. Greenhalgh ES. Structural Power Composites: Future Challenges and Outlook. Gordon Research Conference on Multifunctional Materials and Structures, Ventura, CA, January 2020.
2. Greenhalgh ES., SORCERER - Structural Power Composites for Future Civil Aircraft, AS-09 Clean Sky 2 Research Programme: Developments and Progress, AIAA SciTech 2021, Virtual Event, January 2021.

Poster presentations:

3. Greenhalgh ES, Valkova M, Nguyen S. Structural Power Composites. Gordon Research Conference on Multifunctional Materials and Structures, Ventura, CA, Jan. 2020.

Conference papers in proceedings:

4. Lee C, Panesar A, Greenhalgh E, Design of optimised multi-scale structures for multifunctional composites, ICCM22 Conference, 11-16 August 2019, Melbourne, Australia.
5. E. A. Senokos, D. B. Anthony, S. N. Nguyen, A. R. Kucernak, E. S. Greenhalgh, M. S. P. Shaffer, Manganese Dioxide Decorated Carbon Aerogel/Carbon Fibre Composite as a Promising Electrode for Structural Supercapacitors, ICCM22 Conference, 11-16 August 2019, Melbourne, Australia.
6. S. N. Nguyen, A. Millereux, A. Pouyat, E. S. Greenhalgh, M. S. P. Shaffer, A. Kucernak and P. Linde, Structural Power Performance Requirements for Future Aircraft Integration, ICCM22 Conference, 11-16 August 2019, Melbourne, Australia.
7. E. S. Greenhalgh, M. S. P. Shaffer, A. Kucernak, D. B. Anthony, E. Senokos, S. Nguyen, F. Pernice, G. Zhang, G. Qi, K. Balaskandan, M Valkova, Future Challenges and Industrial Adoption Strategies for Structural Supercapacitors, ICCM22 Conference, 11-16 August 2019, Melbourne, Australia.
8. M Valkova, E. S. Greenhalgh, M. S. P. Shaffer, A. Kucernak, Modelling the Compaction of Hybrid Multi-layer Woven Composite Reinforcement Stacks, ICCM22 Conference, 11-16 August 2019, Melbourne, Australia.
9. D. B. Anthony, S. N. Nguyen, E. Senokos, A. Bismarck, E. S. Greenhalgh and M. S. P. Shaffer, Hierarchical Carbon Aerogel Modified Carbon Fibre Composites for Structural Power Applications, ICCM22 Conference, 11-16 August 2019, Melbourne, Australia.

Popular Science publications:

10. ES Greenhalgh, LE Asp, D Zenkert, J Vilatela, P Linde, En route to ”mass-less” energy storage with structural power composites, JEC Magazine, November, 2019, pp. 37-39.
11. Blog entry, Energy storage in multifunctional carbon fiber composites, Composites World, 1/28/2019.
12. D. Oberhaus, The Batteries of the Future Are Weightless and Invisible, Wired, November 2020, https://www.wired.com/story/the-batteries-of-the-future-are-weightless-and-invisible/
13. Clean Sky 2 announces program updates, G. Nehls (ed), Composites World, November 2020, https://www.compositesworld.com/news/clean-sky-2-announces-program-updates.

Journal papers:

14. Nguyen S, Anthony DB, Qian H, Yue C, Singh A, Bismarck A, Shaffer MSP, Greenhalgh ES, 2019, *Mechanical and physical performance of carbon aerogel reinforced carbon fibre hierarchical composites*, **Composites Science and Technology**, Vol: 182, ISSN: 0266-3538.
15. Asfaw HD, Shaffer MSP, Kucernak ARJ, Greenhalgh ES, *Design of High-Performance Structural Supercapacitors Using Carbon Aerogel-Reinforced Spread Tow Carbon Fibre Fabrics*, **Journal of Power Sources**, 2021, In preparation.
16. Senokos E, Shaffer MSP, Kucernak ARJ, Greenhalgh ES, *CNTs-decorated carbon fibre electrodes for structural supercapacitors: from charged nanocarbon dissolution to high performance device*, 2021, In preparation.
17. Qi G, Nguyen S, Anthony DB, Kucernak ARJ, Shaffer MSP, Greenhalgh ES, *Research Challenges for Fabrication of Structural Supercapacitor Devices*, **Multifunctional Materials**, 2021, Submitted.
18. Shirshova N, Shaffer MSP. *Structural electrolytes: using multifunctional block-copolymers to control the properties of epoxy-IL formulations, Multifunctional Materials*, 2021, In preparation.
19. Pernice MFP, Qi G, Senokos E, Anthony DBA, Nguyen S, Valkova, M, Greenhalgh ES, Shaffer MSP, Kucernak ARJ, *Mechanical and electrochemical characterisation of CFRP/carbon aerogel structural supercapacitor and the corresponding monofunctional equivalents*, **Composites Science and Technology**, 2021, In preparation.
20. Lee C, Greenhalgh E, Shaffer M, Panesar A, *Optimized microstructures for multifunctional structural electrolytes*, **Multifunctional Materials**, 2019, 2, 045001. ISSN: 2399-7532.
21. Valkova et al. *Current collection strategies for structural power composites*, **J Electrochemical Society**, 2021, In preparation.
22. Valkova M et al. *Predicting the compaction of hybrid multilayer woven composite reinforcement stacks*, **Composites Part A**, 2020, p. 105851.
23. Valkova M et al. *Predicting the mechanical response of structural power composites*, **Composites Part C**, 2021, In preparation.
24. Zhang G et al. *Modelling of Structural Supercapacitor towards Understanding the Performance and Influencing Factors*, **Journal of Power Sources**, 2021, In preparation.
25. Johannisson W., Nguyen S., Lindbergh G., Zenkert D., Greenhalgh E., Shaffer M., Kucernak A., *A residual performance methodology to evaluate multifunctional systems*, **Multifunctional Materials**, Vol 3(2), 2020, 025002 https://doi.org/10.1088/2399-7532/ab8e95 (open access)
26. Nguyen SN, Millereux A, Pouyat A, Greenhalgh ES, Shaffer MSP, Kucernak ARJ, Linde P. *Conceptual multifunctional design, feasibility and requirements for structural power in aircraft cabins*, **AIAA J Aircraft**, 2021, Vol. 58, No. 3, pp. 677-687.
27. Nguyen SN, Karadotcheva E, Greenhalgh ES, Shaffer MSP, Kucernak ARJ, Linde P. *Structural power performance targets for future electric aircraft*, **Energies**, 2021, In preparation.
28. Nguyen SN, Ishfaq A, Greenhalgh ES, Shaffer MSP, Kucernak ARJ, Linde P. *Multifunctional design, feasibility and requirements for structural power composites in future air taxis*, **Energies**, 2021, In preparation.